UCRL-16093

University of California

Ernest O. Lawrence Radiation Laboratory

PHOTOIONIZATION OF ALKALI-METAL VAPORS

Berkeley, California

UCRL -16093

UNIVERSITY OF CALIFORNIA

Lawrence Radiation Laboratory
Berkeley, California

AEC Contract No. W-7405-eng-48

PHOTOIONIZATION OF ALKALI-METAL VAPORS

Yuan-tseh Lee
(Ph.D. Thesis)

June 1965

PHOTOIONIZATION OF ALKALI-METAL VAPORS

Yuan-tseh Lee

Inorganic Materials Research Division,
Lawrence Radiation Laboratory,
Department of Chemistry,
University of California, Berkeley, California

ABSTRACT

June 1965

The vapors of potassium, rubidium, and cesium have been photoionized with light absorbed in the discrete region of the atomic spectrum. The energy threshold for the ionization process has been determined and the ions produced identified by mobility measurements. The data give lower limits for the dissociation energies of K_2^+, Rb_2^+ and Cs_2^+. Each of these molecular ions has a bond energy approximately 50% greater than that of the corresponding neutral molecule. In addition, lower limits for the electron affinities of the alkali atoms and values for the mobilities of Rb^+, Rb_2^+, Cs^+ and Cs_2^+ in their present vapor are given.

I. INTRODUCTION

It has long been known[1-4] that the vapors of cesium and rubidium can be photoionized by the light that is absorbed in the discrete region of the atomic spectrum and has energy less than the atomic ionization energy. The very thorough investigations of Mohler and Boeckner[3,5] on cesium vapor showed that the ionization definitely involves the line absorption by cesium atoms, that the rate of ionization is proportional to the first power of the absorbed light intensity, that the phenomenon is independent of temperature, and apparently is not an artifact of the space-charge detector used to measure the ionization currents. Furthermore, they showed that the pressure dependence of the quantum yield of ionization can be represented by the expression.

$$\frac{1}{\Phi} = A + \frac{B}{P}$$

where A and B are constants, and P is the pressure of cesium vapor. These observations suggested that the mechanism of the ionization process is

$$Cs + h\nu \rightarrow Cs^*(nP)$$

$$Cs^* \rightarrow Cs + h\nu \qquad (1)$$

$$Cs^* + Cs \rightarrow Cs_2^+ + e \qquad (2)$$

It is clear that if this analysis is correct, a measurement of the longest wave length at which reaction (2) occurs can be used to calculate a lower limit for the dissociation energy of Cs_2^+. According to Mohler and Boeckner,[3] sensitized ionization first occurs at 3888 A, which suggests the dissociation energy of Cs_2^+ is at least 0.7 eV. Similar experiments

by Freudenberg[4] indicate, however, that the dissociation energy of Cs_2^+ is as high as 1.05 eV. Both these values are larger than 0.45 eV, the dissociation energy of the neutral cesium diatomic molecule, and suggest that the one electron bond in Cs_2^+ is stronger than the two electron bond in Cs_2. This unique order of bond energies for the diatomic alkali molecules was predicted in 1935 by James.[6] More recently, spectroscopic work by Barrow and coworkers[7,8] has been interpreted to mean that the diatomic molecule ions of lithium, sodium, and potassium do indeed have greater bond energies than the diatomic molecules.

Besides reaction (2), there is another process that can lead to photoionization at energies less than the ionization energy:

$$Cs^* + Cs \rightarrow Cs^+ + Cs^- \qquad (3)$$

If this were the exclusive process, the difference between the atomic ionization energy and the appearance energy for ions would be a lower limit for the electron affinity for cesium. Thus the qualitative interpretation of the experiments of Mohler and Boeckner is in some doubt.

Our purpose of this study is to reinvestigate the photoionization of cesium to resolve the disagreement in the earlier work, to identify the ions formed, and to extend these measurements to the other alkali metal vapors.

The special features of collisions between excited atoms and molecules are treated in general in Sec. II. The experimental arrangements and the results of the study of photosensitized ionization of alkali molecule-ions are described in Sec. III. In Sec. IV, the chemical

bonding of alkali molecule-ions is considered. The study of transport phenomena of molecule and atomic ions of rubidium and cesium is given in the last section.

II. COLLISIONS OF EXCITED ATOMS AND MOLECULES

When any molecule passes another at any distance at any relative velocity, if there is a significant exchange of energy, momentum or mass, a "collision" is said to take place. The best description of a particular collision is to give the relative velocity v before the collision and perpendicular distance b between the center of the second molecule and the line of the velocity v through the center of the first. We may call this a (v,b) collision. For a (v,b) collision, there is a probability P(v,b) that a given process may occur on such a collision. The values of P(v,b) must be expected to vary differently with v and b for different transition processes. For statistical purposes we resort to an artifice which gives a convenient index number with which to describe the statistical average over all values of b. We can calculate easily the total number of collisions of relative velocity v within a distance Q, say, denote it by $Z(v, \pi Q^2)\, dv$ and, by equating this to the total number of collisions actually known by experiment to produce the given process, evaluate πQ^2, and call it "the effective velocity cross-section for a given process". Likewise, an "effective temperature cross-section for a given process" which is usually denoted by σ and simply called "effective cross section" can be easily evaluated on the basis of the Maxwellian distribution of velocities along the lines of classical kinetic theory. In this section the statistical index numbers, "effective cross section","mean life of excited state", and "mean time between collision" will be used to discuss the special features of the collisions of excited atoms.

A. Collision Probabilities of Excited Atoms

For an atom which was excited at time t=0 to some excited state of mean life τ, the probability that the excited atom will remain at time t is $\ell^{-t/\tau}$. In a collision process which is characterized by mean time of collision T, the probability that the excited atom will not have made a collision at time t is $\ell^{-t/T}$. The probability that the atom undergoes collision within the time t and t + dt is

$$\ell^{-t/T} - \ell^{-(t+dt)/T} = \ell^{-t/T} \frac{dt}{T}$$

So the probability that an atom will collide in the time between t and t+dt while still in the excited state must be

$$\ell^{-t/T} \ell^{-t/\tau} \frac{dt}{T} = \ell^{-(T+\tau)t/T\tau} \frac{dt}{T}$$

By integrating this equation from t=0 to t= ∞, we can obtain the probability that an atom will collide while still excited as following:

$$P = \int_0^\infty \ell^{-(T+\tau)\, t/T\tau} \frac{dt}{T}$$

$$= - \frac{\tau}{T+\tau} \left[\ell^{-(T+\tau)t/T\tau} \right]_0^\infty$$

$$= \frac{\tau}{T+\tau}$$

This simple relation is often used to evaluate the cross section of the collision process involving excited atoms. For example, in quenching collisions, the quenching Q is defined as the ratio of the intensities of resonance radiation with and without foreign gas. Here, "collision"

means the excitation energy of an atom is transferred to a molecule as the consequence of the encounter of the excited atom with the molecule. Since every quenching collision removes the excitation energy of an atom, in the absence of radiation diffusion and collision broadening,

$$Q = 1 - \frac{\tau}{T+\tau} = \frac{T}{T+\tau} = \frac{1}{1+\tau/T}$$

$$= \frac{1}{1+\tau Z} .$$

This is the famous Stern-Volmer formula, where $Z = 1/T$, the number of collisions for each excited atom in unit time, and can be related to a cross section σ by

$$Z = \frac{2n_1\sigma}{\pi}\sqrt{2\pi\ kT\ (\frac{1}{m_1}+\frac{1}{m_2})}$$

where n_1 is the number of molecules per unit volume and m_1, m_2 are the masses of molecule and excited atom.

B. Types of Collisions

Among the collision processes of excited atoms, there are many processes which are in common with normal atoms, such as upward excitation, or ionization by photons, electrons, atoms or molecules. We are considering those processes which are specific to excited atoms.

According to the consequences of the collisions of the excited atom, the collisions between excited atoms and molecules can be divided into two groups: physical and chemical quenching processes. In the first group we have the following:

1. Photon emission--line broadening.

The pressure dependent line broadening is the consequence of the collision of excited atoms. The line broadening due to the interaction

with atomic particles may be considered to arise from the following cause. Elastic scattering of the atoms both before, after, and during the radiation process is to be expected; but the interaction potential of the excited and unexcited atoms with their neighbors is, of course, different. The radiative process takes place in a time short compared with the scattering process, so that, as with the Franck-Condon principle in diatomic molecules, the radiative transition is nearly vertical. Since the two interaction potentials are "not parallel", a distribution of vertical transition energies will be found; this implies a distribution of radiated frequencies.

Excited atoms in metastable states for which dipole radiation is forbidden have very long mean life times (inverse of transition probability), approximately 10^{-3} -1 sec, or nearly 10^{5} - 10^{8} times larger than those of ordinary excited states. Although dipole transition is not possible, a metastable atom may radiate during a collision with another atom, provided that a suitable state of the quasi-molecule can be found and if radiation from quasi-molecule states is to be allowed. This phenomenon is known as collision induced radiation. It is not an effective process of the destruction of metastable states. For He 2^1S in collision with ground state He atoms, the appropriate quasi-molecule states are $2^1\Sigma_u$ and $2^1\Sigma_g$, of which the latter can radiatively pass to $^1\Sigma_g$. Burhop and Marriott,[9] using the 2^1S ground-state potential energy curves calculated by Buckingham and Dalgarno[10] calculated a mean quenching cross section of $\sigma = 0.9\times10^{-25}$ cm^2 at 300°K. This very low value is due to the barrier which appears in these potential energy curves, but even if this was absent the mean cross section would

only be 5×10^{-22} cm^2.

2. Collisions of the second kind.

In 1921 Klein and Rosseland,[11] on the basis of thermodynamic reasoning, inferred that if ionizing and exciting collisions (collision of the first kind) take place in an assemblage of atoms and electrons, inverse processes must also take place, namely, collisions between excited atoms and electrons in which the excitation energy is transferred to the electrons in the form of kinetic energy. They call such collisions "collisions of the second kind". Now the expression "collision of the second kind" is generally used in a much broader sense, including all collision processes in which the following conditions are fulfilled.[12]

(a) One of the colliding particles is either an excited atom (metastable or otherwise) or an ion.

(b) The other colliding particle is either an electron, a normal atom or a normal molecule.

(c) During the collision, either all or a part of the excitation of particle (a) is transferred to (b).

Collisions of the second kind play an important role in the processes of energy exchange between atoms and molecules. If small quantities of foreign gases are added to the vapor of mercury or sodium, and the sodium or Hg photoexcited, a reduction of the intensity of resonance fluroescence will always be observed. This phenomenon is called the quenching of the fluorescence, and is due to the following causes. During the collision with atoms or molecules of foreign gases, the excited mercury or sodium atoms transfer their excitation energy

and return to their ground state without radiation. The efficiency of quenching is quite different for different gases. In Fig. II-1, are shown the results of the study of the quenching of fluorescence of mercury vapor.[13] It is obvious that rare gases — He, Ar — have little quenching effect, and although a nitrogen molecule possesses only small quenching efficiency, air, CO, O_2 and H_2 possess very high quenching efficiencies.

The detailed theoretical and experimental studies of these and similar phenomena lead to the following important results. The probability of transfer of excitation energy into kinetic energy of collision pairs is very small. The closer the energy levels of colliding atoms or molecules to the energy of the excited atom, the larger the probability of transfer of energy by a collision of the second kind. From these reasons, the rare gases have only small efficiency in the quenching of resonance fluorescence of mercury since the excitation energy of $He(6^3P_1)$ is known to be 4.9 eV, but the lowest excitation energy of helium is about 20 eV. From the same reasons we can understand why molecules always have larger quenching efficiency than atoms. In the case of atoms the only possible energy levels correspond to electronic excitation, and there are relatively few cases in which different atoms have very close energy levels. On the contrary, for molecules, besides electronic energy levels, there are vibrational and rotational energy levels, and the multiplicity of energy levels is much larger. The especially high quenching efficiency of H_2 can be explained by the following facts. The dissociation energy of H_2 is 4.34 eV, and the excitation energy of Hg (6^3P_1) is close to 4.9 eV, so that during

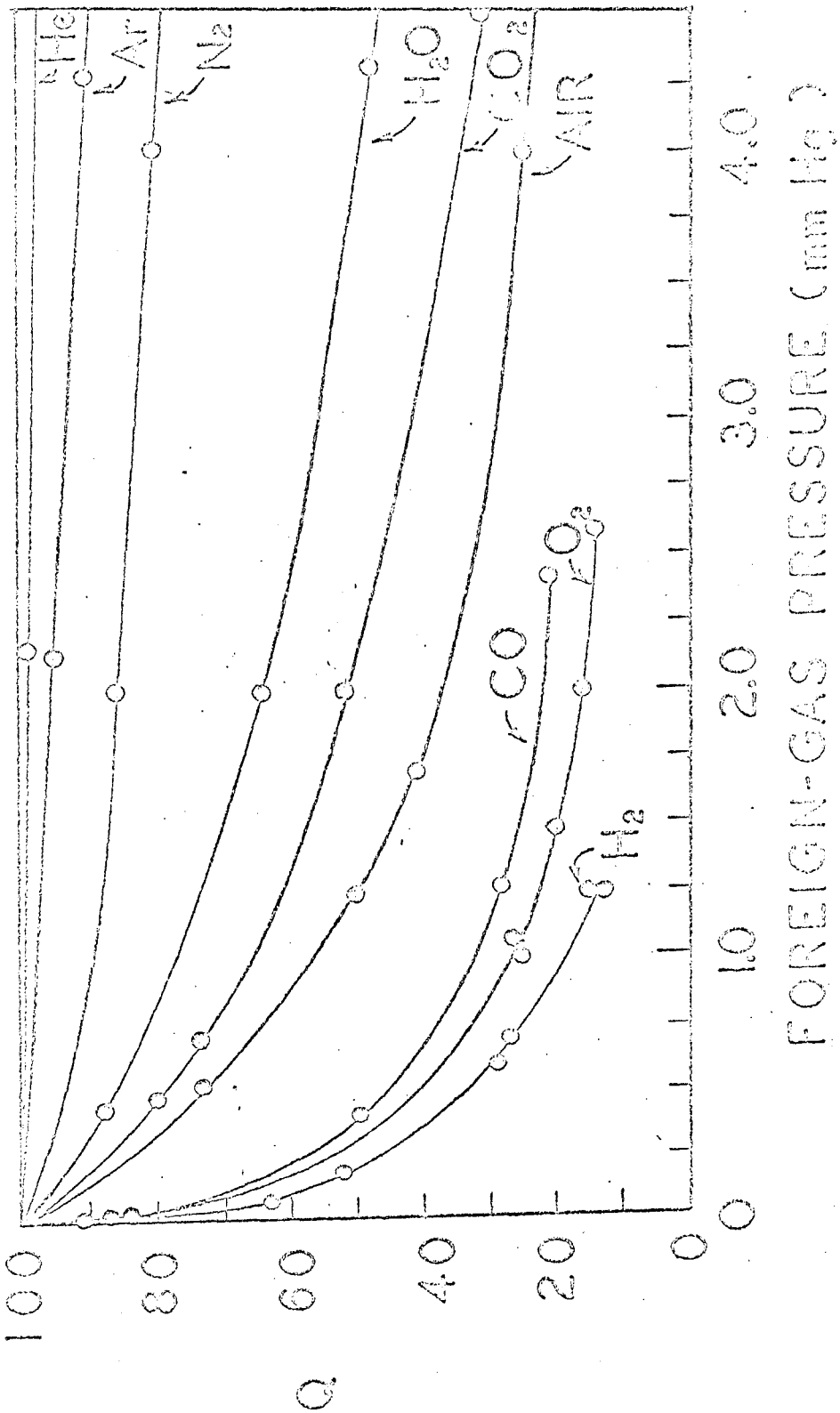

Fig. II-1. Quenching curve for Hg resonance radiation

the collision of the second kind between Hg (6^3P_1) and H_2, the latter can accept the energy which is larger than its dissociation energy with large probability. In fact, Franck was able to show the dissociation of H_2 by observing the appearance of atomic hydrogen, while the mixture of H_2 and mercury vapor was illuminated by the resonance line of mercury.

If we experimentally determine the pressure dependence of quenching, we can calculate the effective cross-section of energy transfer during a collision of the second kind as was shown above. These calculations lead to the following remarkable conclusions. Generally speaking, the effective cross section of a collision of the second kind is several times larger than a gas kinetic cross section (which is usually determined by the phenomena of diffusion, viscosity, etc.). Especially if there is a resonance between the energy of the excited atom and the excitation energy (in extreme cases, dissociation energy and ionization energy), we can always find a sharp increase in the cross section. In the above example of quenching of fluorescence of mercury vapors, the effective quenching cross section of air is 1.8 times the gas kinetic cross section, and that of H_2 is 5.5 times the kinetic cross section.

Resonance phenomena in collisions of the second kind can be shown clearly from the experiment of "sensitized fluorescence" conducted by Beutler and Josephy.[14] They were able to show that, other things being equal, the process was most probably for the smallest energy defect. The excitation of numerous Na levels by Hg (6^3P_1) and to a lesser extent Hg (6^3P_0) is shown in Fig. II-2. Among those excited states of a sodium atom lying between 103 and 113 Kcal/mole ($^2D_{5/2,3/2}$ states with principle

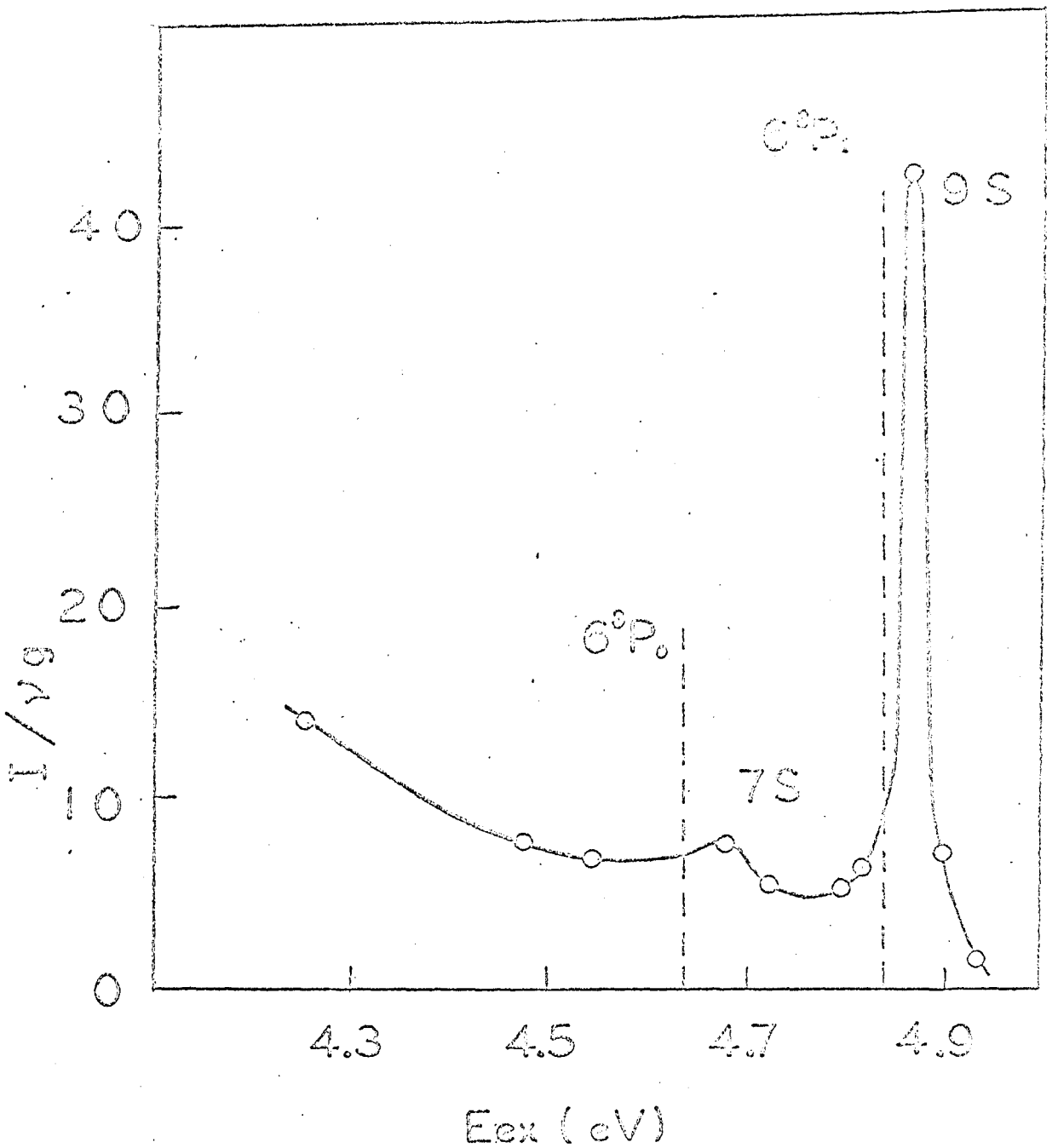

Fig. II-2 Intensity of emission, divided by frequency and statistical weight, in arbitrary units, for levels of Na excited by mercury 6^3P_1 and 6^3P_0, as a function of energy of the Na level.

quantum number from 6 to 9, $^2S_{1/2}$ states with principle quantum number 7 to 10), the $9^2S_{1/2}$ state of sodium was observed to be excited with the greatest probability. The excitation energy of this term is 112.49 Kcal/mole compared to 112.04 for Hg ($^3P_1$). The "resonance" nature of the collision is apparent.

If the excitation energy of the excited atom is higher than the ionization potential of the colliding particle, the transfer of energy may cause the ionization. This is called Penning ionization and will be discussed with other ion producing processes later.

In the chemical quenching processes we have the following:

(3) Formation of molecules

In the presence of a third body, collision of an excited atom with another atom may cause formation of a molecule. For metastable atoms, collision-induced radiation can be relatively unlikely, and the molecule formation process has been invoked to explain high-pressure deactivation of He (2^1S) in helium. The three-body combination process for He (2^3S) in collision with two ground state helium atoms has been reported by Phelps,[15] who observed the resulting $He_2(3^3\Sigma_u^+)$. This molecule has a lifetime of at least 0.05 sec.

(4) Molecule ion formation.

(5) Electron transfer - ion pair production.

(4) and (5) are the two-body processes which are found responsible for the ion production of the present study of the photosensitized ionization of alkali metal vapors. These two processes together with Penning ionization will be described in the next paragraph.

C. Ionization Processes

1. Penning ionization: $X^* + Y = X + Y^+ + e$

If the excitation energy of X^* is higher than the ionization energy of Y, this type of reaction can be a priori expected. Although the important role of this process in ionization phenomena in gaseous mixtures has been known for a long time, the knowledge of these processes is so far very limited.

Recently many experiments have been carried out on Penning ionization, including the single collision beam experiment by Muschlitz and Shollette.[16] Only He 2^3S, 2^1S Ne ^3P are involved in all of these experiments. From these experimental results, comparison may be made between the Penning ionization and the momentum transfer cross section σ_d, usually unknown experimentally, but calculable. It is found the $\sigma_P/\sigma_d \sim 0.2$, a factor comparable with the electron ejection coefficient ξ, for metastables incident upon metal surfaces. Orders of magnitude of σ_P may be estimated thus.

A similar process of collision between excited atoms, $X^* + X^* \rightarrow X + X^+ + e$, has a higher cross section, which is of the order of 10^{-14} cm^2.[17]

The importance of the Penning ionization in gas discharges can be shown from the analysis of a binary mixture of helium and argon by Biondi. If we start with pure helium at a given discharge current and neglect the effect of collisions between excited atoms, the discharge current is the result of direct ionization:

$$He + e^- + \text{kinetic energy} \rightarrow He^+ + 2e^-$$

Simple energy considerations indicate that in order to produce an electron-ion pair the bombarding electron must have an energy in excess of 25 eV.

If, however, some argon is introduced, Penning ionization may take place:

$$He + e^- + k.e. \rightarrow He^* \text{ (metastable)} + e^-$$

$$He^* \text{ (metastable)} + A \rightarrow He + A^+ + e^-$$

Here the energy required to produce an electron-ion pair is that to produce a helium metastable, or $\geq$ 20 eV. Thus for a given degree of ionization (discharge current) a smaller discharge voltage is required when argon atoms are present.

With pure helium, in order to maintain the discharge current there must be a sufficient number of electrons in the high field energy tail of the distribution to create helium ions and electrons. However, with argon present, the same rate of ionization can be maintained by electrons which have only enough energy to create metastable helium atoms. As a result the electron distribution is substantially altered over the energy range in which the excited levels of helium lie.

Thus, as argon is added to helium the helium lines emitted decrease markedly as a result of the downward shift in the tail of the electron distribution. The net result is that the argon/helium ratio inferred from the ratio of characteristic line intensities is much greater than the true argon/helium ratio.

2. Molecular ion formation.

The formation of molecular ion XY^+ in a reaction $X^* + Y \rightarrow XY^+ + e$

by a two body collision is made possible by the fact that the electron released carries away the heat of reaction in the form of kinetic energy and thus stabilizes the molecular ion XY^+.

This particular case of chemical ionization is sometimes called the Hornbeck-Molnar process as a credit to their first thorough examination of the formation of molecular ions of noble gases in a mass spectrometer in 1951. The proper explanation of this ionization process was in fact given as early as in 1928 by Franck,[18] and was verified by Mohler and Boeckner in the study of the formation of Cs_2^+ in 1930.[19]

As is true for other elementary reactions occurring in highly energized systems, our knowledge of this process is still very limited. Full understanding is required by recent developments of radiation chemistry, gaseous electronics, plasma physics, and reaction kinetics in flames. More attention has been paid recently to these fields.

Precise measurement of the appearance potential of each of the molecular ions produced is one of the most important things in the study of this process. The studies of this process have been concentrated on noble gases so far, but the information obtained is only limited to the appearance potentials. The appearance potentials of six independent studies of homonuclear and heteronuclear molecular ions of noble gases are listed in Table II-1.

All of the experiments in Table II-1 were carried out in a mass spectrometer. In the first five columns, the measured appearance potentials are involved with uncertainty of errors of 0.1 eV or more, which is related to the energy spread of electron beam. In the last column the appearance potentials were measured by using the retarding

Table II-1. Appearance Potential of Molecular Ions of Noble Gases

Ions	Appearance Potential in Volts					
	1.	2.	3.	4.	5.	6.
He_2^+	$23.18^{+0.2}_{-0.7}$		23.4	$23.08[^3P]$	23.3±0.1	
Ne_2^+	$20.86^{+0.3}_{-0.7}$				20.9±0.2	
Ar_2^+	$15.05^{+0.2}_{-0.7}$				14.7±0.1	14.94±0.02
Kr_2^+	$13.23^{+0.3}_{-0.7}$		13.2		13.0±0.1	13.20±0.02
Xe_2^+		11.7	11.6		11.2±0.1	
$HeNe^+$			22.6		23.4±0.1	
$He\ A^+$					17.9±0.3	
$He\ K^+$					19.9±0.1	
$Ne\ Ar^+$					16.8±0.1	
$Ne\ Kr^+$					16.6±0.1	
$Ne\ Xe^+$					16.0±0.3	
$Ar\ Kr^+$					14.0±0.1	
$Ar\ Xe^+$			13.5		13.5±0.1	
$Kr\ Xe^+$			12.2		12.3±0.1	

1. J. A. Hornbeck, J. P. Molnar, Phys. Rev. 84, 62 (1951).
2. F. H. Field, J. L. Franklin, Symposium on Mass Spectrometry, Oxford 1961.
3. V. W. Kaul, R. Taubert, Z. Naturforsch. 17a, 88-89 (1962).
4. F. J. Comes, Z. Naturforsch. 17a, 1032-33 (1962).
5. M. S. B. Munson, J. L. Franklin, F. H. Field, J. Phys. Chem. 67, 1542 (1963).
6. C. E. Melton, N. H. Hamill, J. Chem. Phys. 41, 1471 (1964).

potential method. In this experiment, the investigators were able to resolve some of the excited states which contribute the formation of molecular ions. Recent developments in the field of electron energy selection, electrostatic electron energy selector, or the retarding potential method, will enable the workers in this field to carry out more precise measurements. In column 4, the appearance potential of He_2^+, 23.08 eV, is not the datum of direct measurement. Comes' measurement gave 23.1±0.3 eV. There are six excited states of helium lying within his experimental error. There are 3^1S[22.92 eV], 3^1P[23.09 eV], 3'D[23.08 eV], 3^3S[22.72 eV], 3^3P[23.01 eV], 3^3D[23.08 eV]. By comparison of the curve form of the He_2^+ ion current as a function of voltage with the known excitation function of He, Comes excluded all three singlets. Since among those three triplets, 3^3P has the highest probability of excitation, he concluded that 3^3P is responsible for the appearance of He_2^+.

In those heteronuclear ions, appearance potentials are higher than the ionization potentials of one of the atoms. These facts indicate that the molecular ion formation process may effectively compete with Penning ionization.

More information about the nature of this process and chemical bonding of molecular ions would be obtained if the kinetic energy of the ejected electrons were measured. Preliminary experiments in these directions were reported to have been commenced.[20]

Molecular ion formation processes play many important roles in a highly energized system. Recently, Bogdanova and Geitsi[21] showed that an additional maximum appeared close to the threshold on the optical excitation functions of some lines of helium if hydrogen, krypton, or mercury vapor was added

to the helium. No additional maximum was observed when neon was added. Further study of Bogdanova and Bochkova[22] discovered that the process which produced the additional maximum is a process of "delayed" excitation of atomic levels involving appearance and subsequent decay of molecular ion formation. Since dissociative recombination leads to the selective excitation of atoms, the additional maximum is not observed on the optical excitation functions of all the helium lines. The role of the impurity (H_2, Kr, Hg) is secondary, as was confirmed by direct measurements—it leads to the appearance of slow electrons that facilitate the dissociative recombination.

This process is one of the practical methods to determine the lower bound of dissociation energy of some of the molecular ions, since the lower bound of the dissociation energy of molecular ion is related to the difference between the ionization potential of the atom and the appearance potential of the molecular ion. The detailed energy cycles will be found in Sec. III.

3. Electron transfer--ion pair production.

The ion pair production processes, $X^* + Y \rightarrow X^+ + Y^-$, are usually observed in collisions between atoms of high kinetic energy. Since the lowest ionization potential of the atom of a naturally occurring element, 3.893 eV for Cs, is higher than the highest electron affinity of a normal atom, 3.7 eV for Cl, electron transfer from normal atom to neutral atom cannot be expected in the collision processes of thermal energy.

In the collisions of excited atoms, electron transfer is energetically possible if the difference between the ionization potential and excitation energy of the atom is smaller than the electron affinity of the collision

partner. Recently, Melton and Hamill[23] reported experimental study of the electron transfer from excited krypton atom to sulfur dioxide and the dissociative electron transfer from excited krypton to carbon tetrachloride to produce Cl^- and CCl_3.

In this particular type of collision process, because the strong Coulomb interaction distorts the potential energy curves in such a way that the pseudo-crossover occurs at a suitable and calculable nuclear separation, the cross section can be calculated for the simple systems by application of the Landau-Zener formula.[24]

Theoretical calculation of the reverse processes, recombination of positive and negative ions, have been carried out on H^-, H^+ by Bates and Lewis,[25] and on H^-, Li^+ by Bates and Boyd.[26] The experimental studies of these collisions will give the most rigid test of the pseudo-crossover theory. The only rate coefficients that have been measured in the laboratory are those for iodine and for bromine ions.

In our experiments, electron transfer processes are observed from highly excited potassium, rubidium, and cesium atoms to normal potassium, rubidium, and cesium atoms. From the difference between the ionization potential and lowest excitation energy which is necessary to undergo an ion pair production process, the lower bounds of the electron affinity of potassium, rubidium, and cesium were estimated.

III PHOTOSENSITIZED IONIZATION OF ALKALI METAL VAPORS

A. Experimental Arrangements

In photosensitized ionization, if the mean time between collisions is much shorter than the mean life time of spontaneous radiation of the excited species, the rate of production of ions is proportional to the rate of production of excited species by resonance absorption, and the latter is always limited by the intensity of effective light which can be obtained conventionally. This condition held in the work to be described.

The block diagram of the apparatus is given in Fig. III-1. The photoionization experiments were carried out in a quartz cell which contained platinum parallel plate electrodes of 3 X 15 cm dimension separated by 3 cm. Light from a 500 watt Osram lamp passed through a chopper, a Hilger D285 monochromator, and a collimating lens and slit system. The parallel light beam of 0.2 X 1 cm cross section passed between the parallel plate electrodes and onto a photomultiplier used to monitor the light intensity. Care was taken to prevent scattered light or photoexcited atoms from striking the electrodes. In virtually all experiments the slit-width of the monochromator was 0.1 mm, which gave a band pass of 10 A or less throughout the spectral region investigated.

During the experiments, the pressure of the alkali metal vapor was controlled by the temperature of the appendix tube, which was heated by a separate oven controlled by a thermister and a proportional control amplifier, and the ionization cell was maintained at a temperature at least 50°C higher than the condensation temperature of the vapor.

In the cell containing alkali metal vapor, because the electrodes are always covered with adsorbed alkali metal, there was a substantial thermionic electron emission. In a new cell this thermal electron current amounted to 10^{-9} amp/cm^2 at 300°C for cesium, and became larger

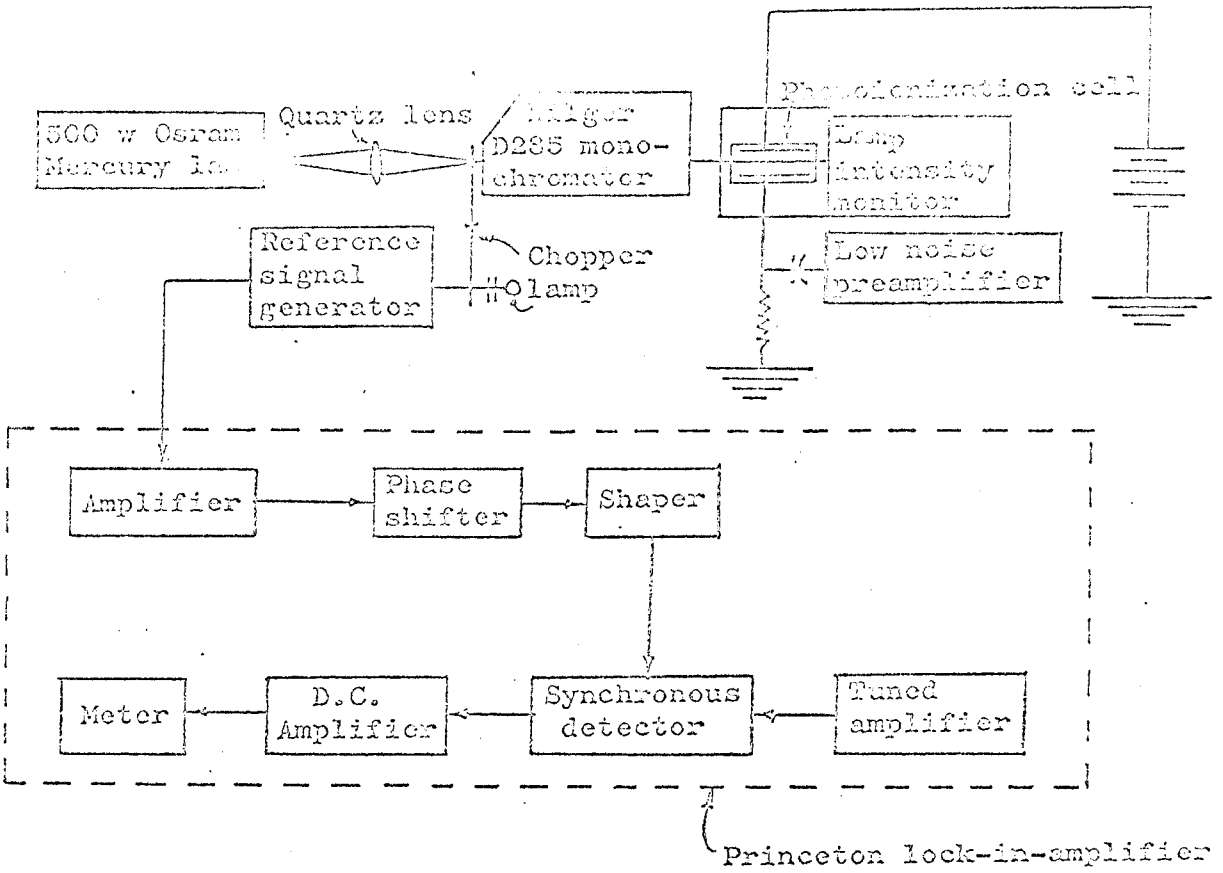

Fig. III-1 Schematic Diagram of the Experimental Arrangement.

as the cell aged and an oxide film began to coat the electrodes. Since this thermal electron current is always larger than the expected photoionization current of 10^{-12} to 10^{-13} amp., the latter was detected by chopping the light and using a narrow band width preamplifier followed by a Princeton Applied Research lock-in amplifier.

In preliminary experiments, in order to measure the photoionization current directly by using a vibrating-reed electrometer, an attempt was made to suppress the thermionic electron emission from the collector by surrounding the latter with a fine grid. But due to the high thermionic electron emission from the grid itself, we were not able to reduce the background current to the order of the magnitude of photoionization current.

B. Construction and Filling of the Cell

The main chamber of the photoionization cell was made of a 6 cm o.d. X 16 cm long quartz tube. Both ends were sealed with 1/16 inch optical quartz plates as the windows of the cell. A side arm of 12 mm o.d. was connected to the main chamber. The length of the side arm was 22 cm from the center of the chamber. Besides the electrodes, the only non-quartz parts were the four Kovar-glass seals of the electrode leads.

Two 3 X 15 cm platinum sheets with a thickness of 0.005 inch were mounted to nickel frames and each of the latter was supported by two 0.060 inch Kovar rods. Before the assemblage, these electrodes were heated in the hydrogen oven at a temperature of 1000°C. This treatment markedly reduced the thermal emission of electrons from the electrode surfaces and was essential to the suppression of space charge effects and improvement of signal to noise ratio. Immediately before filling, the reaction cell was prepared by evacuation to less than 10^{-6} torr and baking at 350°C for at least 24 hours. An ampoule of the alkali metal

was opened in an evacuated side tube isolated from the cell by a liquid nitrogen trap, and the metal refluxed so that it could act as a getter for traces of oxygen remaining in the cell. Finally a sample of the metal was distilled into an appendix tube whose temperature could be controlled independently of the temperature of the photoionization cell.

The side view of the cell and the filling system is given in Fig. III-2.

The potassium, rubidium and cesium used in this research were obtained from commercial suppliers and had a purity of 99.8% or better.

C. Light Source

A 500 watt Super Pressure Osram lamp was used in most of the experiments. It is similar to General Electric AH-6, operated at 100 atms and gives a continuous spectrum ranging from visible down to 2900 A accompanied by broadened mercury lines. Since the light source of the Osram lamp is concentrated in the very small volume of a sphere of 0.5 cm diameter, the intensity of light emitted from the unit area is much larger than from a 1000 watt AH-6.

In order to study the threshold of photosensitized ionization, we prepared electrodeless microwave discharge lamps of rubidium and cesium. They consisted of a 10 mm o.d. X 10 cm quartz tube with an end window containing alkali metal and krypton. The enhancing effect of the emission of resonance lines from alkali metal vapor by introduction of noble gas is well known.[27] Before introducing alkali metal and krypton, the quartz tube was cleaned by repeated discharge with fresh krypton of 2 mm Hg and then thoroughly evacuated and baked out. The most satisfactory results were observed between 1.5 mm Hg to 2.0 mm Hg. The lamps were usually fired in a microwave resonant cavity with the consumption of 50 watts of

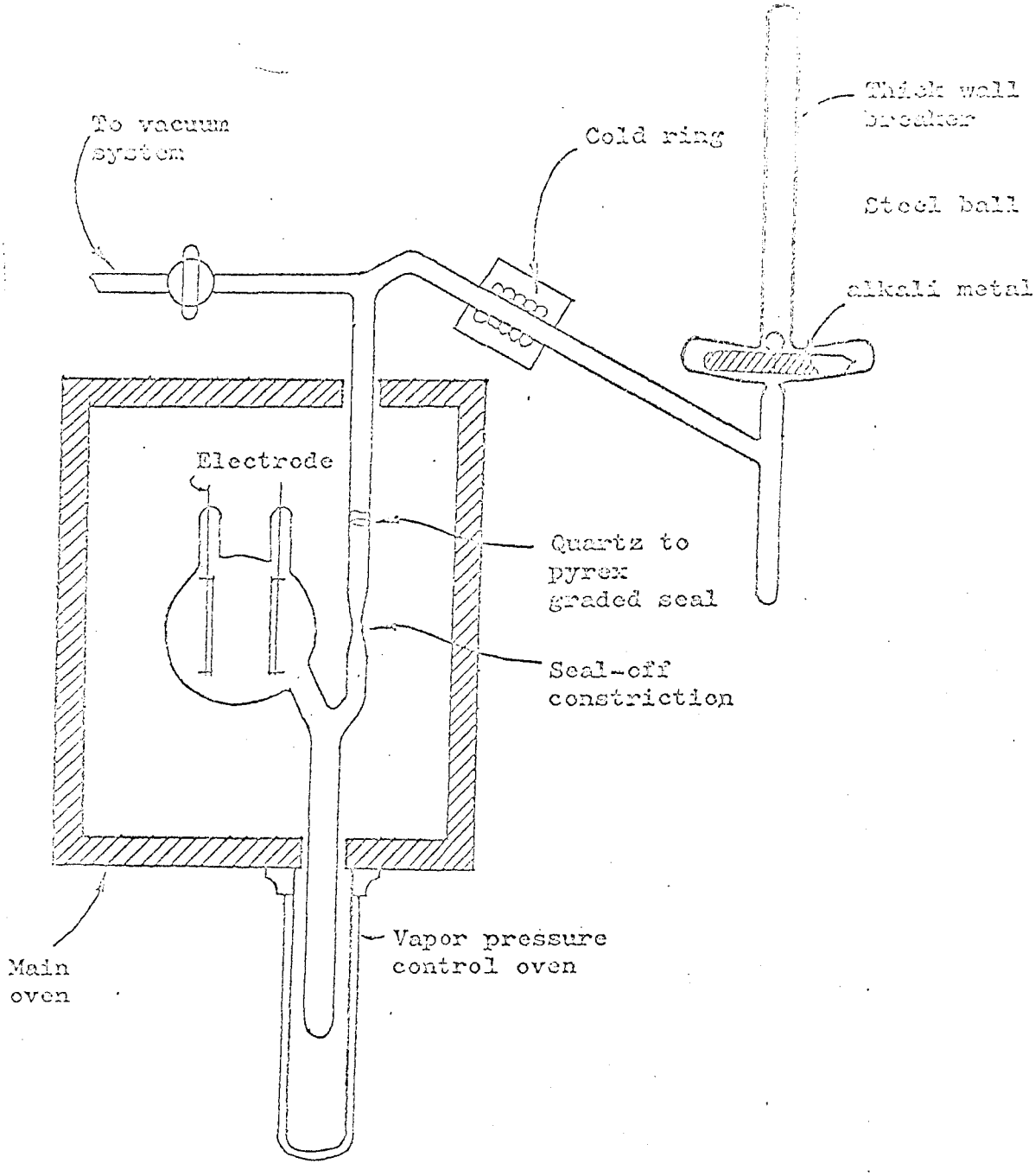

Fig.III-2 Side view of the photoionization cell and alkali metal filling system.

power. The intensity of light emitted is several times larger than that from an ordinary spectroscopic lamp of comparable power, and the stability of the lamp is better too. Ordinarily the light emitted from a resonance lamp is concentrated in the first few resonance lines. In our lamps the intensities of the first three resonance lines are stronger than that of the equivalent part of the 500 watt Osram lamp.

A similar electrodeless He lamp was used to excite the Cs atom into the $8P_{1/2}$ state, since the strong helium line 3888.6A coincides with one of the doublet components of the third member of the principal series in cesium, 3888.6A ($6\ S_{1/2}$-$8\ P_{1/2}$). The advantage of this source is that it gives a strong exciting line exhibiting no self-reversal.

D. Identification of Different Ions

In order to obtain information about the nature of the sensitized ionization process, it is necessary to identify the collected ions. We attempted to identify the ions produced photolytically by use of a radiofrequency mass spectrometer. This experiment failed, however, because of the copious field emission of electrons from the spectrometer electrodes. A more convenient way to distinguish between Cs_2^+ and Cs^+, for example, is by measurement of the mobilities of the photo-ions. According to the recent work of Chanin and Steen,[28] the mobilities of Cs_2^+ and Cs^+ in cesium vapor are 0.21 and 0.075 cm/volt-sec respectively at a density of 2.69×10^{19} atoms/cc. The mobility of the atomic ion Cs^+ is small because of the large cross-section for resonant charge exchange collisions in the parent vapor. Consequently, reaction (2) [$M^* + M \rightarrow M_2^+ + e$] should produce ions of relatively high mobility, while reaction (3) [$M^* + M \rightarrow M^+ + M^-$] should give ions of low mobility.

In the mobility measurements, photo-ions were produced in a well localized thin rectangular band parallel to the electrodes. Since the width of the ion-producing region is only about 1/20 of the migration distance of the ions, by chopping the light beam with a suitable frequency, the mobility can be calculated from the measured phase shift between the exciting light and the collected plate current.

At a cesium pressure of 0.1 torr, a temperature of 300°C, and a field strength of 7 volts/cm, the migration velocity of the ions are such that the phase angle between the exciting light and the collected plate current is measurable if the chopping frequency is 1.4×10^{3}/sec. The interpretation of the phase shift in terms of absolute mobilities is difficult, however, because of the presence of the space-charge limited thermal emission from the negative plate. Any positive ions produced in the gas neutralize some of the space charge during their migration to the collecting electrode and cause an increased electron current which amplifies the ion signal and reduces the apparent phase angle between the exciting light and the ion current. Therefore, the measured phase angle between the exciting light and current always corresponds to an absolute mobility that is too small by some unknown factor that depends on space charge effects.

From highly excited states, it is quite probable that the two reactions (2) and (3) compete. Consequently the collected ion current might be the composition of two signals with different phase shifts. In order to prevent the cancellation of amplitude and to keep a simple relation between the composition and the phase shift of the composite signal, care was taken to carry out the experiments under conditions such

that the difference between the phase shifts of X_2^+ and X^+ was about 90°.

E. Experimental Results

1. Threshold energies of photosensitized ionization.

For potassium, rubidium, and cesium, sensitized photoionization was observed for at least nine wavelengths that correspond in each case to discrete lines in the principal series absorption ($nS\text{-}mP_{1/2,3/2}$) of the atom. More lines could be resolved by using a smaller slit-width in the monochromator. For each of the alkali metal vapors, the sensitized ionization threshold corresponded to the excitation of the $(n+2)P$ state, where n is the principal quantum number of the valence electron in the ground state of the atom. The wavelengths at the sensitized ionization threshold, the corresponding energies, the true ionization energies of the atoms, and the difference between atomic ionization energies and sensitized ionization threshold energies, are summarized in Table III-1.

Our data confirm the results of Mohler and Boeckner that the threshold wavelength for cesium is 3888 A. We were unable to detect any ionization produced by absorption of the 4555 A line of Cs, in contrast to Freudenberg. From the following cyclic relations, it is obvious that the difference between the atomic ionization potential and the sensitized ionization threshold will give us the lower limits for either the bond energy of the molecule ion or the electron affinity of the atom, depending on the mechanism of reaction of the excited species, since for reaction (2) $[M^* + M \rightarrow M_2^+ + e]$ and (3) $[M^* + M \rightarrow M^+ + M^-]$ to occur, ΔE must be larger than or approximately equal to zero, and at the threshold the value of ΔE will be the lowest. The energy required for the reaction to

Table III-1. The wavelengths at the sensitized ionization thresholds, the corresponding energies, the atomic ionization energies and the difference between atomic ionization energies and sensitized ionization threshold energies of potassium, rubidium, and cesium.

	K	Rb	Cs
Chemi-ionization threshold, A	3447	3591	3889
Threshold energy, eV	3.59	3.45	3.19
Atomic ionization energy, eV	4.34	4.18	3.89
Difference, eV	0.75	0.73	0.70

proceed in the forward reaction is noted on the side of the arrow.

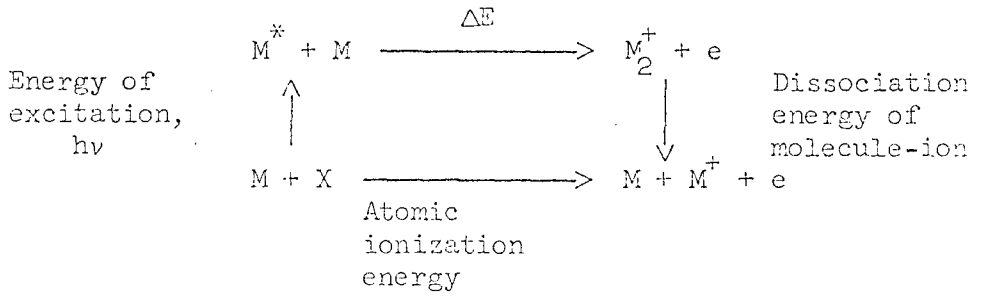

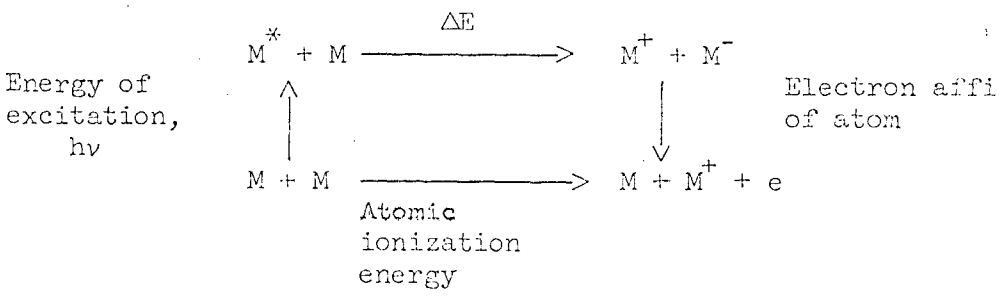

Our data show that the bond energy of the molecule ion or the electron affinity of the atom is at least 0.75, 0.73, 0.70 eV for potassium, rubidium, and cesium respectively, but probably not higher than 1.15,

1.21 or 1.25 eV, since no photosensitized ionization was observed from the excitation of the (n+1)P states.

2. Nature of Photosensitized Ionization Process.

Measurement of the phase angle as a function of the wave length of the exciting radiation does provide information about the nature of the sensitized ionization process, even though absolute mobilities are not determined at this stage. Figure III-3 shows that the phase angle between the light and the collected current is the same for the three lower absorption lines of Cs. Thereafter the phase angle increases as successively higher states are excited, and reaches a constant maximum at the series limit and beyond. Since the measured phase angle corresponds to the migration time of the ions and is inversely proportional to the mobility of the ion, one interpretation of these data is that excitations to the states below 12P lead predominately to molecular ions, and that states above 12P lead to increasing amounts of positive and negative atomic ions via process (3). If this interpretation is accepted, the data show the bond energy of Cs_2^+ is at least 0.70 eV, but probably not higher than 1.15 eV, and the appearance of atomic ions at the 12P level indicates the electron affinity of cesium is at least 0.19 eV.

It should be noted that Mohler and Boeckner[3] were able to measure $\sigma\tau$, the product of the collision cross section for ionization and the lifetime of the excited states of the cesium atom, as a function of excitation energy. They found $\sigma\tau$ is constant for states up to 14P, and then increases abruptly for higher states. Their ionization efficiency curves measured from saturation currents indicate that the quantum yield of ions increases abruptly for states above 13P. Both these observations

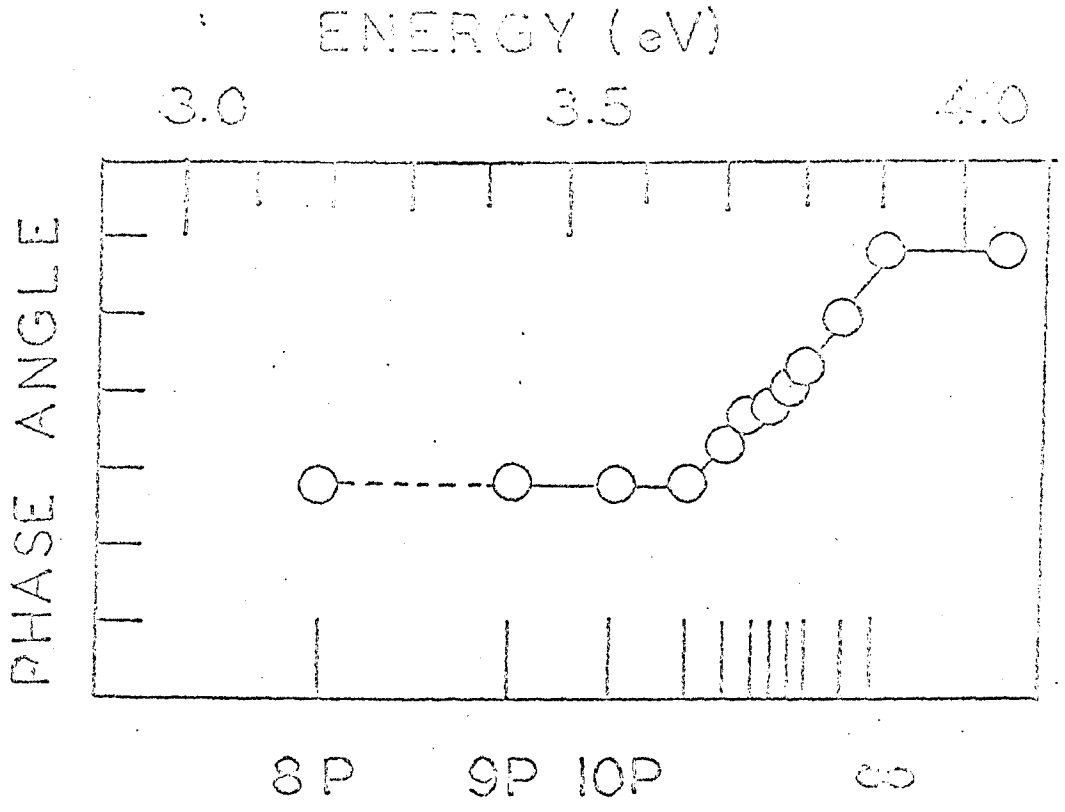

Fig. III-3 Phase angle (arbitrary units) as a function of photoexcitation energy for the cesium system. Experimental conditions: 6.67 volts/cm, 339 C, 0.15mm Hg. Ionization from the 8P state could be detected, but its phase could not be measured.

suggest that a second ionization process has its onset somewhere above the 12P level.

Measurements of the phase angle as a function of wavelength were also performed with rubidium vapor, and the results are shown in Fig. III-4. As was true for cesium, the first four states that chemi-ionize give a high-mobility ion, in this case presumably Rb_2^+. Excitations to states above 10P lead to ions of lower mobility in an amount that increases with excitation energy. The bond energy of Rb_2^+ is thus at least 0.73 eV, but probably not higher than 1.21 eV, and the electron affinity of Rb is at least 0.20 eV.

The mobility experiments were repeated using potassium vapor, and the data collected are shown in Fig. III-5. Because of the low volatility of potassium, it was necessary to use moderately high temperatures (390°C) in the ionization cell. At these temperatures, the windows of the cell tended to discolor, and this in turn reduced the light intensity and made the measurements difficult. For this reason it was not possible to measure the phase angle associated with excitations near to and above the ionization limit. For the other lines, the phase angle increases and the mobility decreases as the excitation energy increases. There is a plateau of constant mobility for the lower states, as was observed for rubidium and cesium. This suggests that in potassium vapor, both molecular ions and positive-negative atomic ion pairs are produced from excitations to the 8P state and higher levels. The excitation to the 7P level must at least produce molecular ions, and therefore it is likely that the excitations to the 6P level also lead to molecular ions, and perhaps atomic ion pairs as well. Thus the bond energy of K_2^+ is at least 0.75 eV and

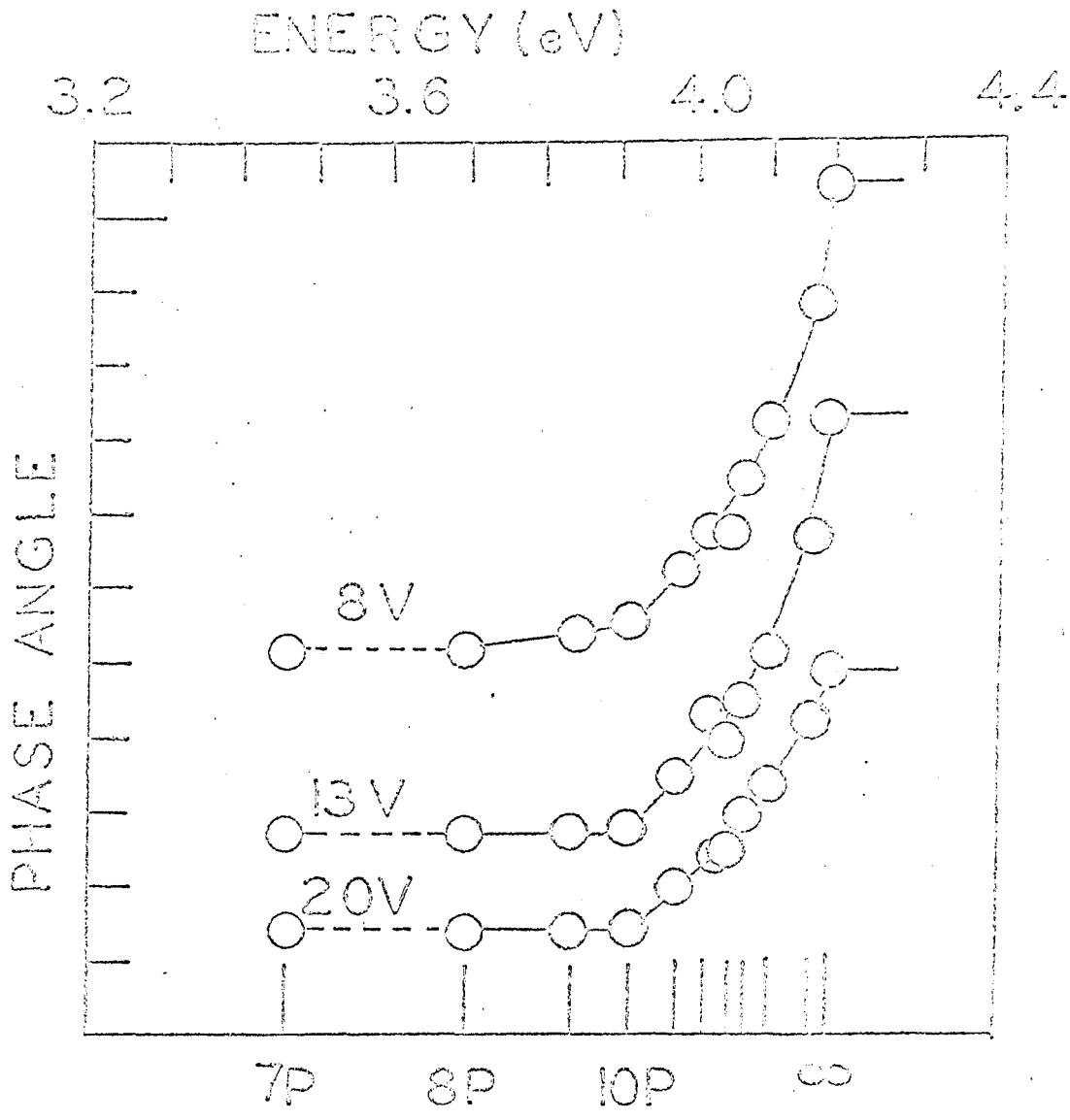

Fig. III-4 Phase angle (arbitrary units) as a function of photoexcitation energy for the rubidium system. Experimental conditions: Voltage as indicated, 339 C, 0.125 mm Hg. Ionization from the 7 P state coud be detected, but its phase could not be measured.

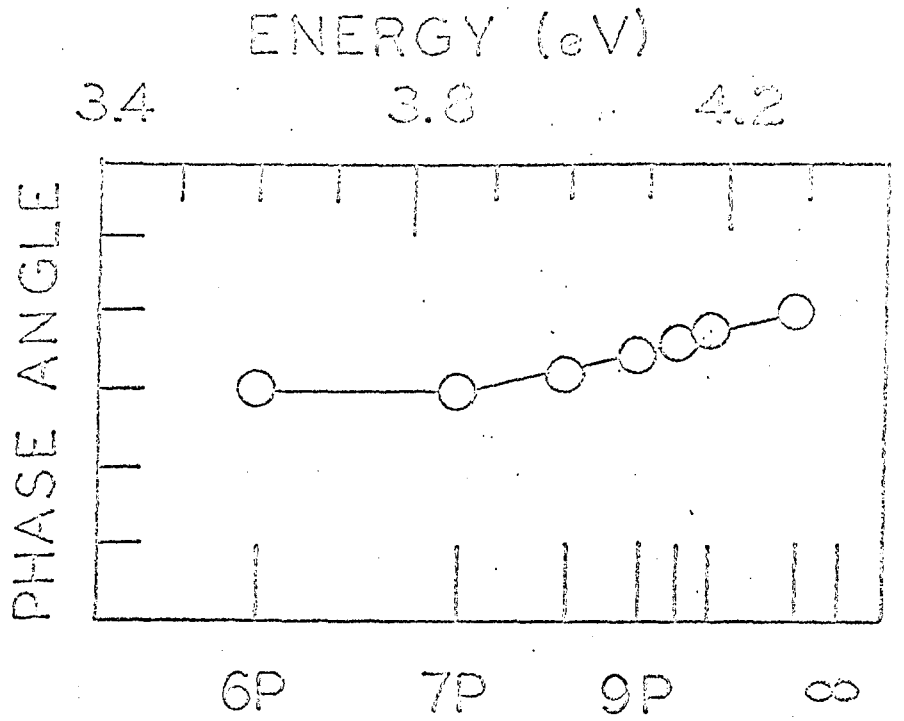

Fig. III-5 Phase angle (arbitrary units) as a function of photoexcitation energy for the potassium system. Experimental conditions: 2.67 volts/cm, 300 C, 0.068 mm Hg.

probably not higher than 1.25 eV. The lower limit of bond energy is very close to the value of 0.76 eV estimated from spectroscopic work of Robertson and Barrow. The lower limit of the electron affinity of potassium may be 0.35, 0.49, or 0.75 eV, depending on whether negative ions are first produced from the 8P, 7P, or 6P state respectively.

Table III-2 lists the dissociation energies of the alkali metal molecules and molecule ions. The spectroscopic work of Barrow yields the ionization energy of the alkali molecule directly, and this quantity must be combined with the ionization energy of the atom and the dissociation energy of the molecule to give the dissociation energy of the molecule ion. Our own measurements combined with the atomic ionization energies give the lower limits for the bond energies directly, and are not subject to possible uncertainties in the bond energies of the molecules. The data make it clear that, contrary to the assertion of Pauling, the bond energies of the alkali molecule ions are greater than those of the alkali molecules.

The atomic ion and molecule ion can also be distinguished from the measurement of the ion current as a function of electric field. This is given for Rb_2^+ and Rb^+ in Fig. III-6. Since the space charge multiplication of the signal is not constant during the migration of the ion toward the electrode, the quantitative analysis is difficult. The more rapid increase of ion current of Rb_2^+ as a function of electric field is credited to the greater mobility of Rb_2^+. The detailed discussion of the mobilities of alkali metal ions in their parent gases will be given in Sec. V. The decrease of ion current at higher electric field is due to the decrease of the space charge multiplication effect.

Table III-2. Dissociation Energies of Alkali Molecules (eV)

	$De(M_2)$	$De(M_2^+)$
Li	1.12[a]	1.55[b]
Na	0.73[c]	1.01[b]
K	0.514[c]	0.75 ~ 1.25
Rb	0.49[c]	0.73 ~ 1.21
Cs	0.45[c]	0.70 ~ 1.15

[a] D. Wagman, W. Evans, R. Jacobson, T. Munson, J. Res. Nat. Bur. Standards, 55, 83 (1955).

[b] Reference 33

[c] G. Herzberg, Spectra of Diatomic Molecules, 2nd. Ed., D. Van Nostrand Co., New York, 1950.

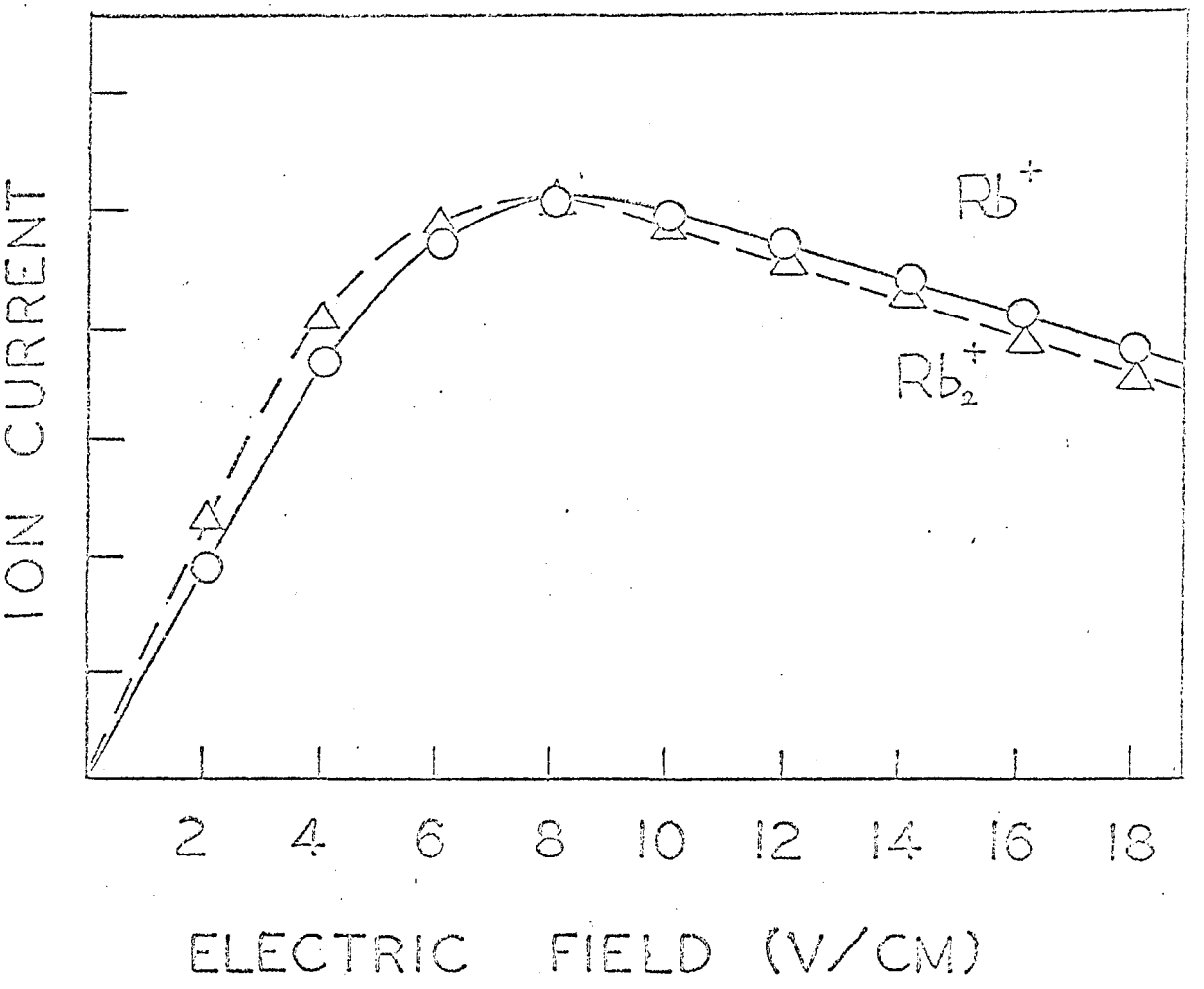

Fig. III - 6. Ion current (arbitrary scale) as a function of electric field. Experimental conditions: 301°C, 0.03 mm Hg.

3. The ratio of M^+/M_2^+ as a function of the excitation energy

It is possible to estimate the ratio M^+/M_2^+ as a function of the excitation energy of the colliding atoms. This can be done if it is assumed that at the threshold of chemi-ionization, only M_2^+ is produced, and beyond the ionization limit only M^+ is formed, for then the phase ϕ of the signal due to M^+ relative to that of M_2^+ can be established. If we define the phase detection angle Θ such that the M_2^+ signal is a maximum when $\Theta = \Pi/2$, we have

$$I_{M_2^+} \propto \sin \Theta$$

$$I_{M^+} \propto \sin(\Theta-\phi)$$

$$I_{total} \propto [\sin \Theta + A \sin(\Theta-\phi)]$$

where I is the detected signal, and A is the relative amplitude of the signal due to M^+. To maximize the detected signal, we chose a detection angle Θ_m such that

$$\left[\frac{dI}{d\Theta}\right]_{\Theta_m} = 0 = \cos\Theta_m + A \cos(\Theta_m-\phi)$$

$$A = -\frac{\cos \Theta_m}{\cos(\Theta_m-\phi)}$$

Thus measurement of Θ_m and knowledge of ϕ allows calculation of the relative amounts of M^+ and M_2^+ produced by a given excitation. The result is subject to the assumption that the response of the detector is the same for M_2^+ and M^+, and this may not be strictly true because of space charge effects. The attendant error is probably less than 50%, and would correspond to an overestimate of M^+ production. The results for the Rb and Cs systems are given in Table III-3. The increase in

Table III-3. Fractional Yields of Monatomic Ions

	$Rb^+/(Rb^+ + Rb_2^+)$	$Cs^+/(Cs^+ + Cs_2^+)$
8P	0	-
9P	0.031	0
10P	0.031	0
11P	0.16	0
12P	0.24	0.17
13P	0.32	0.30
14P	0.40	0.33
15P	-	0.43
16P	0.52	0.50
∞	100	100

the importance of the atomic pair process relative to molecule ion formation is an interesting and perhaps unique demonstration of how electronic excitation energy affects the relative cross sections of competing reactions. A complete explanation of this behavior must involve a knowledge of the potential energy curves for the alkali molecules, and this is not yet available.

IV. CHEMICAL BONDING OF ALKALI MOLECULE IONS

A. Evaluation of Bond Energy of Molecular Ions

The direct spectroscopic investigation of molecule ions is extremely difficult, and not much information has been obtained so far from the spectroscopy of molecule ions themselves. The bond energy of molecule ions is usually estimated by the following methods.

(1) Determination of the lower bound from the difference between the ionization potential of atoms and the appearance potential of molecule ions in atomic gases or vapors.

This method is used in this work and was mentioned in Sec. III. From the cyclic relation on page 29 it follows that,

$$D_o(M_2^+) \geq I(M) - A.P.(M_2^+)$$

where A.P. is the appearance potential of X_2^+, or the minimum excitation energy to produce molecular ions.

(2) Analysis of scattering data

An estimate of the interaction energy of an ion and an atom can be obtained from the scattering cross sections of the atomic ions by atomic neutrals. The general practice is to analyze the scattering data in terms of some potential function, such as the Morse potential, and determine disposable parameters from the scattering data. The process of obtaining a potential curve from scattering data involves several uncertainties so that this result cannot on its own merit be regarded as reliable.

(3) From the energy cycle

$$D_o(M_2^+) = D_o(M_2^*) + I(M^*) - I(M_2^*)$$

M_2^*, M^* might be electronically excited or in the ground state. The term value of M^* must be related to that of M_2^*.

The dissociation energy of He_2^+ quoted in Herzberg's famous "Spectra of Diatomic Molecules" was found from the energy cycle

$$D_o(He_2^+(^2\Sigma_u^+)) = D_o(He^*(^3\Sigma_u^+)) + I(He^*(2^3S)) - I(He_2^*(^3\Sigma_u^+))$$

The last two terms of the right member of the above equation are known with high accuracy. The first term was obtained by means of a linear Birge-Sponer extrapolation of the spectroscopic data.

The dissociation energy of Li_2^+, Na_2^+ and K_2^+ listed in Table III-2 were deduced from this type of energy cycle. As was mentioned in Sec. III, $D_o(M_2^+)$, of lithium, sodium and potassium were evaluated from known $D_o(M_2)$, $I(M)$ together with Barrow's recent spectroscopic determination of $I(M_2)$. Of course the dissociation energy determined in this method is subject to the uncertainty of any of the three members on the right hand side of the equation.

(4) Quantum mechanical calculation

With the help of electronic computors Ab initio quantum mechanics has now progressed to the point where one can hope to make statements about the dissociation energy of simple molecules which are more accurate than the experimental statements. The variation principle states that a variational calculation of the energy $E_{calc}(R)$ provides a rigorous upper limit for the molecule at the separation R. It follows that the quantity De^{LB}

$$De^{LB} \equiv E_{exp}(\infty) - E_{calc}(Re) \leq De$$

where $E_{exp}(\infty)$ is the sum of the experimental atomic energies, provides a rigorous lower bound to the dissociation energy.

All of these four methods have been used to determine the dissociation energy.

a) Do 1.5 ± 0.3eV[29]

b) De = 2.16eV[30] (De = Do + 0.1)

c) Do $(He_2^+(^2\Sigma_u^+))$ = 3.1eV[31]

d) De^{LB} = 2.24eV[32]

The 3.1 eV obtained by method 3 is believed to be too high, since Do $(He_2^*(^3\Sigma_u^+))$ is obtained by the Birge-Sponer extrapolation of spectroscopic data. The estimates of this type are generally too high.[33] Re[illegible], Browne and Matsen[32] estimated from similar quantum mechanical calculation on more complex systems that the dissociation energy of He_2^+ should be no more than 0.3 eV greater than their calculated lower bound 2.24 eV.

B. General Picture of Alkali Molecule-Ions

From our experimental study on potassium, rubidium and cesium, together with Barrow's spectroscopic work on lithium, sodium and potassium, it is apparent that the dissociation energies of alkali molecular ions, as listed in Table III-2, are at least forty to fifty percent higher than that of corresponding diatomic molecules. Although

these experimental findings cannot be explained by any of the simple concepts of chemical bonding, the quantum mechanical calculations on lithium molecule ion and lithium molecule lead to the same conclusion. The calculation of James[34] in 1935 indicated that the bond energy of Li_2^+ should be greater than that of Li_2, and on the basis of an analysis of this result, James predicted that a similar relation should hold for the other alkali molecules and their ions. A more recent calculation on Li_2 is the SCF LCAO MO six-electron treatments of Faulkner.[35] This calculation as in the other molecular orbital calculations gave rather poor results (0.33 eV) for the computed Dissociation energy [rationalized dissociation energy = $E_{calc}(\infty) - E_{cal}(R_e)$], mainly because of the error in $E_{calc}(\infty)$. However, the calculated total molecular energy is 0.9920 of the experimental total molecular energy, which is good agreement. The calculated first ionization potential of Li_2, which is expected to be the most accurate of the physical constants calculated, is given by $2\sigma_g$ orbital energy, and is 0.48 volt less than the experimental first ionization potential of atomic lithium. This indicates that the bond energy of Li_2^+ is 0.48 eV greater than that of Li_2, which is in good agreement with the experiment.

No direct information about the bond lengths of alkali molecular ions has been obtained so far, but we can figure out some qualitative features from the knowledge of the electronically excited alkali diatomic molecules, since the electronically excited molecules can be considered as a system of molecular ions and a loosely bound electron. Barrow's spectroscopic study indicated that in the electronically excited alkali

diatomic molecules the internuclear distances are larger and the force constants are smaller than those of the ground state neutral molecules. The same things can be expected for molecular ions.

C. Discussion

From the fact that the one-electron bond in the hydrogen molecule-ion is about half as strong as the electron-pair bond in the hydrogen molecule (Do = 60.95 Kcal/mole for H_2^+, 102.62 Kcal/mole for H_2); and, since the same number of atomic orbitals is needed for a one-electron bond as for an electron-pair bond, Pauling suggested that, in general, molecules containing one-electron bonds will be less stable than those in which all the stable bond orbitals are used in electron-pair bond formation. Consequently he proposed that the internuclear distances of alkali molecule-ions are about 0.3 A greater than for the corresponding normal states and that the bond energies are about 60 percent of those for the corresponding electron-pair bonds. Surprisingly, this simple basic concept of bond order, which has been proved to be useful in the systematic understanding of the chemical bond, leads to an erroneous conclusion on the dissociation energies of these simple alkali molecule-ions. This special phenomenon of alkali molecule-ions apparently is not a general feature of molecule-ions. As we can see clearly from Table IV-1, the dissociation energies of these molecule-ions at the other end of the periodic table agree qualitatively with what we expect from bond order.

Table IV-1 Dissociation energies of some of the diatomic ions

Dissociation energy (D) (Kcal/mole)	O_2^+	149	O_2	117	F_2^+	76[a]	F_2	37[c]	Ne_2^+	15[d]
					Cl_2^+	97[b]	Cl_2	58[c]	Ar_2^+	19[e]
					Br_2^+	64[b]	Br_2	46[c]	Kr_2^+	18[e]
					I_2^+	54[b]	I_2	36[c]	Xe_x^+	12[f]
No. of Valence electrons										
bonding	8		8		8		8		8	
Antibonding	3		4		5		6		7	
Bond Order	2 1/2		2		1 1/2		1		1/2	

a) R. P. Iczkowski and J. L. Margrave, J. Chem. Phys. 30 403.

b) Calculated from A. P. data in F. H. Field and J. L. Franklin "Electron Impact Phenomena"

c) S. W. Benson, "The Foundations of Chemical Kinetics" Appendix C.

d) Calculated from A. P. data in Table II-1, column 5.

e) Calculated from A. P. data in Table II-1, column 6.

f) Calculated from A. P. data in Table II-1, column 3.

James[34] attributed the unusual order of bond strengths to the repulsions involving the inner shell electrons that are more important in Li_2 than in Li_2^+. The integrals associated with this repulsion involve exchanges of inner and outer shell electrons, and thus do not have a simple classical interpretation.

Sinanoglu and Mortensen[36] discussed the importance of core polarization by valence electrons on the bond energy of Li_2. The calculated core polarization energy for the 2S electron in lithium atom is about 0.102 eV, and the core polarization energy between one lithium core and a σ2S electron in Li_2 is about 0.062 eV. They concluded that core polarization lowers the total energy of the Li_2 molecule and its separated atoms by essentially the same amount (Li_2; 4 X 0.062 = 0.248 eV, 2Li; 2 X 0.102 = 0.204 eV) and thus does not make an important contribution to the bond energy. In Li_2^+, the core polarization energy is not known. The average distance between the σ2S electron and one of the lithium cores in Li_2^+ is larger, however, than the average distance between the 2S electron and the lithium core in the lithium atom. We can therefore expect that the core polarization energy between the σ2S electron and one of the lithium cores in Li_2^+, as in the case of Li_2, is not larger than the core polarization energy for the 2S electron in the lithium atom. This means that the contribution of core polarization to the bond energy cannot exceed 0.1 eV, and is too small to account for the higher bond energy of Li_2^+. The general conclusion drawn from the model of core polarization, that explicit inner-outer shell interactions are not important would seem to be in conflict with the conclusions of James.[34]

In recent theoretical calculations on some excited states of He_2^+, Browne[37] established from the computed potential energy curves that those states that originate from the interaction of a bare helium nucleus and a neutral helium atom are bound, and those states that separate into a pair of ground state helium ions, and into $He^+(1S) + He^+(2S)$ are not bound. The comparison of the potential energy curves of these bound states with the curves resulting from classical polarization leads to the conclusion that these bound states are primarily due to polarization effects rather than to the traditional chemical mechanism. A similar conclusion has also been reached about LiH^+, the bond energy being explained as a result of polarization of H by Li^+. In ordinary molecule ions, such as those given in Table IV-1, the polarization interaction between ions and atoms, which can be roughly estimated from the polarizability of the atom and the interatomic distance using the classical polarization interaction equation, is much smaller than the bond energy which can be expected from the bond order and the known dissociation energy of corresponding neutral molecules. This means that polarization interactions only play a secondary role, and chemical mechanisms contribute primarily to the dissociation energy of these molecules. For alkali molecule ions, due to the large polarizability of the alkali atom, the classical polarization energy is larger than the "bond energy" that can be expected from bond order. For example, in a system of Cs^+ and Cs, the polarization interaction energy is 0.7 eV at an interatomic distance of 4.8 A, which is the approximate bond length of Cs_2^+ and is 0.3 A longer than that of Cs_2. On the other hand the bond energy that can be expected from bond order is

less than 0.3 eV. The classical polarization interaction might not give an accurate estimation for the polarization interaction between atom and ion in a short distance, but it shows that in alkali molecule-ions the factor which is considered to be secondary in the simple model of the chemical bond, is comparable to or even more important than the primary factor on which the simple model of the chemical bond was built. This situation is also true for other metallic molecule ions of bond order 1/2, such as alkaline earth molecule-ions and molecule ions of zinc, cadmium, and mercury. The dissociation energies of Be_2^+ (2.7 eV[39]) and Hg_2^+(0.9 eV[40]) are also higher than those of Li_2 and Cs_2. The explanation of the complicated molecular energy in terms of simple concepts is difficult, but the classical polarization energy between ion and atom at a distance equivalent to the bond length can be considered as the approximate lower limit of the dissociation energy. In those extreme cases of metallic molecule-ions of bond order 1/2, there is reasonable agreement between classical polarization energy and dissociation energy.

V. MOBILITY OF RUBIDIUM AND CESIUM IONS IN THEIR PARENT VAPORS

The mobility of alkali metal ions in foreign gases, especially in noble gases, has been thoroughly investigated both experimentally and theoretically. But due to experimental difficulties, the mobility of alkali metal ions in their parent vapors has not been studied as thoroughly. Recently the mobility of Cs^+ and Cs_2^+, has been reported by Chanin and Steen, but there are many features that remain to be investigated further. The mobility of Rb^+ and Rb_2^+, in their own vapor is still not available. In this section the study of the mobility of cesium and rubidium ions will be discussed.

A. Experimental Arrangements

As was mentioned in Sec. III, in the cell containing alkali metal vapors there is a constant flow of thermoelectrons from the collector electrode to the repeller electrode. Due to the space charge effect, the thermionic emission of electrons from the collector electrode will be enhanced by the existence of positive ions between the two electrodes. In our experiment it is found that the positive-ion induced electron current is always much higher than the positive ion current itself. Since the emission of one electron from the collector electrode has the same effect as the collection of one positive ion, the collected plate current corresponds to the observation of positive ions in the space between the electrodes rather than to the response to arrivals of positive ions at the collector electrode.

In our experiment, the mobilities of ions were measured by the phase shift between the exciting light and the collected plate current. In order to make the measured phase shift equivalent to the time of

migration of ions, it is necessary to isolate the collector so that it can respond to the collection of positive ions but will not respond to the existence of positive ions in the space between the collector and repeller electrodes. This is achieved by inserting a very fine tungsten screen with high transmission in front of the collector electrode. This fine tungsten screen forms a good equipotential surface and separates the space between repeller electrode and collector electrode into a large migration region, i.e., the space between the repeller electrode and the tungsten screen, and a small detection region, i.e., the space between the tungsten screen and the collector electrode. When the positive ions are produced in the migration region, the thermoelectric current between tungsten screen and repeller electrode will be enhanced by the existence of positive ions which are migrating toward the tungsten screen, but due to the shielding effect of the tungsten screen, the thermionic electron emission of collector electrode will not be affected by the existence of positive ion in the migration region. The collector electrode will first respond to the positive ions when positive ions get through the tungsten screen and arrive at the detection region, and thus we have a well defined migration distance for the ions. The end effect of the detection of positive ions in the detection region due to finite distance between the tungsten screen and collector electrode can be compensated by changing the migration distance for positive ions. This can be achieved by simply moving the oven, and thus changing the distance between the exciting light and the collector electrode.

The construction of the cell for mobility measurement is similar to that of the cell mentioned in Sec. III. The new electrode is a 200 mesh

tungsten screen mounted on a 5.0 X 9.0cm nickel frame, which is placed 5.5 cm away from the repeller electrode and 3 mm away from the collector electrode. The tungsten screen is made of 0.0095 inch wire and has 80% transmission. The repeller electrode has the same dimension as tungsten screen and the 2.0 X 5.5 cm collector electrode is surrounded by a guard ring which is in the same plane as the collector electrode and is 1 mm away from each side of the collector electrode. The outside dimension of the guard ring is 5.0 X 9.0 cm.

The filling of the cell and the experimental procedure are the same as before. In the phase angle measurement, the phase shifter of the lock-in amplifier was adjusted so that the phase shift between collected plate current and reference signal was either $n\pi$ or $(n + 1/2)\pi$. These two cases give maximum and zero reading of the amplifier output, and can also be identified easily and accurately by using the oscilloscope to observe the wave form of the output of synchronous detector of lock-in amplifier. The readings of the phase shift are taken from the phase shifter of the lock-in amplifier and are converted into degrees.

The monoatomic positive ions, Rb^+ and Cs^+, were produced by direct photoionization and the diatomic molecule ions, Rb_2^+ and Cs_2^+, were produced by photosensitized ionization. As was mentioned in Sec. III, the photosensitized ionization from low lying excited states will produce diatomic molecule ions exclusively through reaction (2). To produce diatomic ions we excited atoms into the $(n + 3)P$ state, since the yield of molecule ions from the sensitized ionization threshold, $(n + 2)P$ state, is considerably lower. Under our typical experimental conditions, 0.1 mm Hg and 300°C, most of the excited atoms collide with normal atoms while still excited, and since mean life time of spontaneous

radiation of (n + 3)P state of Rb and Cs is about 10^{-7} sec, the mean time of conversion from excited atoms into molecule ions is no more than 10^{-7} sec. This is 10^{-4} times smaller than the migration time of ions in the cell, 10^{-3} sec, and can be neglected in the mobility measurements. Consequently, we can safely consider the time of production of molecule ions to be the same as the time of illumination of exciting light.

B. Vapor Pressure and Fraction of Diatomic Molecules of Rubidium and Cesium

1. Vapor pressure.

Since there are reliable vapor pressure equations for both rubidium and cesium, the vapor pressure can be calculated from the measured temperature of the appendix tube. No attempt was made to measure vapor pressure directly in our experiments.

The most reliable vapor pressure equation for cesium over a wide temperature range is derived by Kvater and Meister[41] from the measurement of temperature dependence of optical density of resonance doublet by the hook method. The equation is given as:

$$\log P(Cs) = -\frac{3529}{T} + \log T + 3.6572$$

Kvater and Meister's optical density measurement were carried out in the temperature range from 336°K to 553°K, but since the boiling point calculated from this equation, 941°K, agrees very well with the experimentally measured, 943 ± 5°K,[42] we can believe this equation is reliable up to 943°K. Taylor and Langmuir[43] used a surface ionization method and carried out the vapor pressure measurement in the temperature range from 239°K to 346°K, which is just below the temperature range of Kvater and Meisters. This experiment is believed to be the most reliable

measurement in this range, and their data for liquid cesium (T 302°K) agree very well with the Kvater and Meister equation. However their proposed equation for liquid cesium:

$$\log P(Cs) = 11.0531 - 1.35 \log T - 4041/T$$

will give a vapor pressure of 565 mm Hg at the boiling point, which is 27% lower than the expected 760 mm Hg. This demonstrates that although Taylor and Langmuir made an accurate measurement, the proposed equation cannot be applied without substantial error beyond their experimental range.

The following vapor pressure equation for rubidium was derived by Goldberg[44] from the measurement of optical density in the temperature range from 348°K to 553°K.

$$\log P = - 3611.4/T + \log T + 3.61914$$

The extrapolation of this equation to boiling point also gives good results. At the boiling point (969.2°K) this equation gives P = 757.5 mm Hg, which very nearly coincides with the expected pressure P = 760 mm Hg and demonstrates the validity of this equation from 348°K to the boiling point.

Vapor pressure of rubidium and cesium calculated from these equations are given in Fig. V-1.

2. Fractions of diatomic molecules of rubidium and cesium in their vapors.

Rubidium and cesium vapors are mainly composed of monatomic species. The diatomic species have been estimated at no more than 1% of the saturated vapors. In order to facilitate the discussion of our experimental results, which will be given in V-C, we are going to consider the equilibrium constant for formation of diatomic molecule and the concentration of diatomic species in the vapor as a function of temperature.

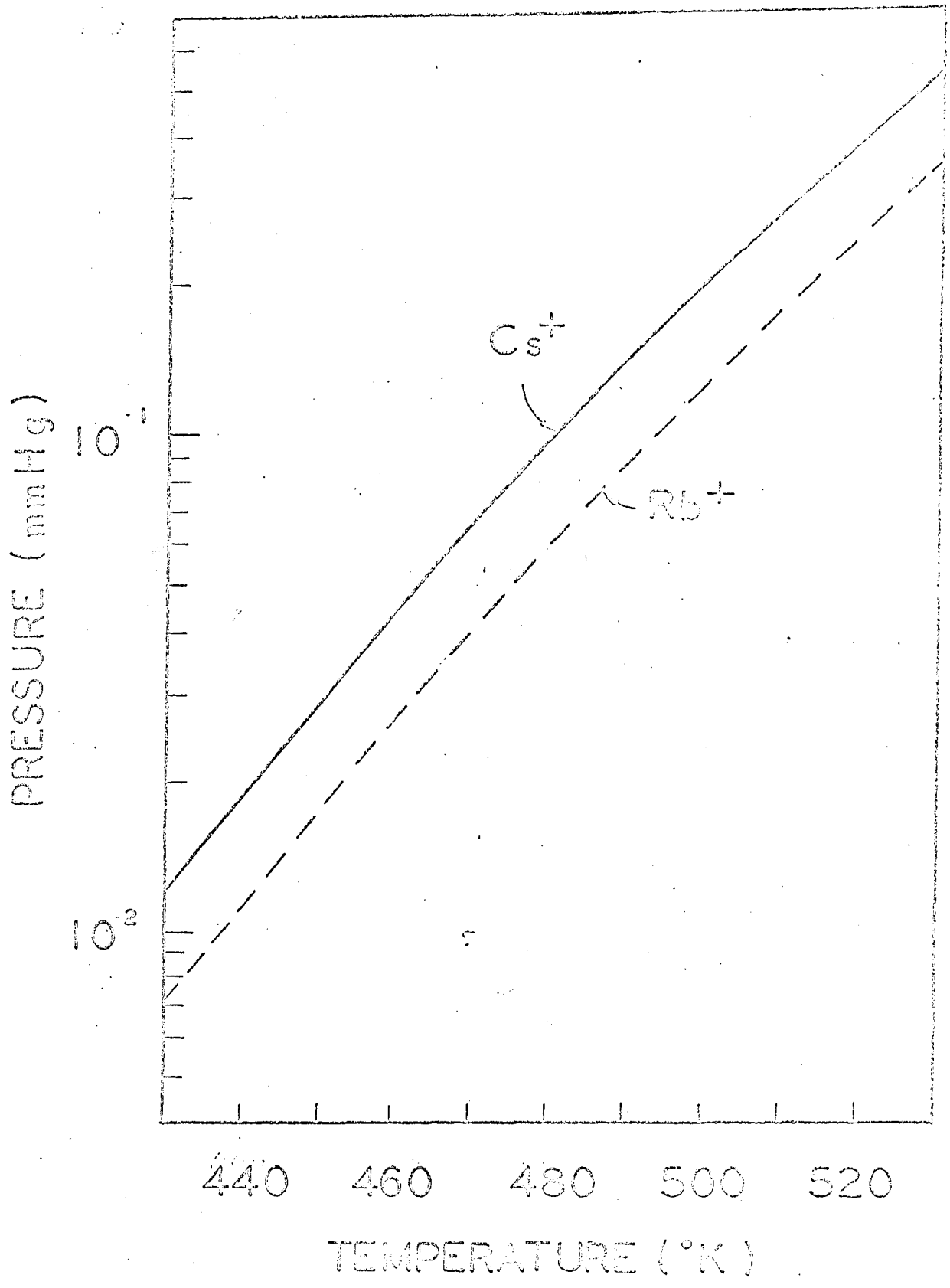

Fig. V-1. The variation of vapor pressures of Rb and Cs with temperature

Evan, Jacobson, Munson and Wagman[45] made an extensive statistical mechanical calculation of the thermodynamic properties of the alkali metals in the naturally occurring isotopic mixtures. In their calculation of the thermodynamic functions of diatomic gases, the rotational and vibrational constants given in Table V-1 were used to calculate the thermodynamic functions for a rigid rotator with moment of inertia, I, equal to $h/[8\pi^2 CB_e(1-\alpha_e/2)]$,[46] and symmetry number 2, and for an independent harmonic oscillator with a fundamental frequency of $(\omega_e - 2X_e\omega_e)$. Then corrections were made to include the effects of rotational stretching, vibrational harmonicity and rotational-vibrational interaction.

The results of their calculation of the equilibrium constants of formation of Rb_2 and Cs_2 in the temperature range from 400 K to 700 K are given in Table V-2 and Table V-3. The fraction of diatomic molecules under the pressures of 10%, 50%, and 100% of the saturated vapor pressure have been calculated by using the equilibrium constants and vapor pressure equations given in B-1. These are also tabulated in Table V-2 and V-3.

Table V-1 Molecular Constants[a] of Alkali Metals

	Li_2	Na_2	K_2	Rb_2	Cs_2
$10^8 r$, cm	2.672_5	3.078_6	3.923	4.12_7[b]	4.46_5[b]
B_e, cm^{-1}	0.67272	0.15471	0.05622	0.0231_5[b]	0.0127_2[b]
α_e, cm^{-1}	0.00702	0.00078	0.000219	0.000058[c]	0.000035[c]
ω_e, cm^{-1}	351.43_5	159.23	92.64	57.28	41.990
$x_e\omega_e$, cm^{-1}	2.592	0.726	0.354	0.096[d]	0.08005
$10^8 D_o$, cm^{-1}	986.	58.4	8.3	1.5[e]	0.47[e]
$10^8 \beta$, cm^{-1}	28.	0.5	0.8	-------	-------

a Values from Herzberg, except as noted.

b Estimated by a Badger's rule extrapolation.

c Estimated from $\alpha = 6B_e^2/\omega_e[(x_e\omega_e/B_e)^{1/2} - 1]$.

d Given erroneously as 0.96 by Herzberg; see Tsi-ze and San-Tsiang and Kusch. [Phys. Rev. 52, 91 (1937): ibid 49, 218 (1935)].

e These values are for $D_e = D_o - 1/2\beta$. Estimated from $D_e = 4B_e^3/\omega_e^2$.

Table V-2. Equilibrium constants of formation of Rb_2 and their fraction in the vapor.

T(°K)	log Kf	$\left(= \frac{P_{Rb_2}}{P_{Rb}^2}\right)$ Kf	Fraction of Rb_2 under different pressures (% of saturation)		
			10%	50%	100%
400	2.7389	5.49×10^{2}	1.12×10^{-4}	5.60×10^{-4}	1.12×10^{-3}
500	1.4528	2.84×10	4.65×10^{-4}	2.33×10^{-3}	4.65×10^{-3}
600	0.589	3.88	1.22×10^{-3}	6.10×10^{-3}	1.22×10^{-2}
700	-0.032	0.929	2.47×10^{-3}	1.24×10^{-2}	2.47×10^{-2}

Table V-3. Equilibrium constants of formation of Cs_2 and their fraction in the vapor.

T(°K)	log Kf	$\left(= \frac{P_{Cs_2}}{P_{Cs}^2}\right)$ Kf	Fraction of Cs under different pressures (% of saturation)		
			10%	50%	100%
400	2.3396	2.19×10^{2}	7.86×10^{-5}	3.93×10^{-4}	7.86×10^{-4}
500	1.1570	1.44×10	3.78×10^{-4}	1.89×10^{-3}	3.78×10^{-3}
600	0.363	2.31	1.09×10^{-3}	5.45×10^{-3}	1.09×10^{-2}
700	-0.206	0.622	2.37×10^{-3}	1.19×10^{-2}	2.37×10^{-2}

C. Results and Discussion

1. Conversion of atomic ions into molecule-ions.

In the measurement of the migration velocities of atomic ions of rubidium and cesium in their parent vapors, the mobility appeared to be constant over a substantial range of ion lifetime. But when the time between production and collection increased, the apparent mobility of M^+ increased. The time that these atomic ions migrated under constant velocities after they were produced was found to be approximately inversely proportional to the density of diatomic molecules in their parent gases. This increase of migration velocity was not observed for the diatomic molecule-ions.

Both the increase of migration velocities and their dependence on the density of diatomic molecules strongly suggested that the atomic ion is converted into fast moving molecule ions through two body process

$$M^+ + M_2 \rightarrow M_2^+ + M$$

since this type of reaction is exothermic in alkali metals and can be expected to be very rapid according to the general theory of ion-molecule reactions.

On the basis of this scheme, we have estimated the rate of conversion under the assumption that the change of migration velocity, as was indicated from the measured phase shift, was first observed when half of the atomic ions were converted into molecule-ions. The density of the diatomic molecule was estimated theoretically, as was mentioned before.

Since in alkali metal vapos the diatomic molecules are in equilibrium with the atoms, and under our experimental conditions the concentration

of neutral diatomic species is very much higher than that of atomic ions, the density of diatomic species is essentially not affected by the ion molecule reaction.

If we assume the concentration of atomic ions is $[M^+]_0$ when it is produced at time t = 0, and if we consider the concentration of diatomic molecules $[M_2]$ is constant, we can integrate the equation

$$-\frac{d[M^+]}{dt} = k[M^+][M_2]$$

into the following

$$\log \frac{[M^+]}{[M^+]_0} = -k\,[M_2]t$$

where $[M^+]$ is the concentration of M^+ at time t.

From the measured time, $t_{1/2}$, for 50% conversion and the knowledge of $[M_2]$, the rate constant

$$k = -\frac{\log 1/2}{[M]t_{1/2}} = \frac{\log 2}{[M]t_{1/2}}$$

can be calculated. The calculated k and the experimental conditions are given in Table V-4.

The rate constants of two-body ion-molecule reactions can be estimated theoretically by finding a critical impact parameter b_o such that, the orbits $b < b_o$ collapse into the center of the force field, until limited by repulsive forces. Using Langevin's classical formulation Gioumousis and Stevenson[47] obtained the relation

$$k = 2\pi \left(\frac{\alpha e^2}{\mu}\right)^{1/2}$$

where α is the polarizability of molecules and μ is the reduced mass. The rate constants calculated from this equation must be regarded as approximate upper limits, since it is not necessary that all of the ions

that collapse into the center of the force field will react with the molecules. Neither experimental nor theoretical data on the polarizability of diatomic rubidium and cesium molecules are available, but from the theoretical study of the polarizability of Li_2, it seems to be reasonable to assume that the polarizabilities of rubidium and cesium molecules are approximately 110 X 10^{-24} cm^3 and 90 X 10^{-24} cm^3, which are about ten percent higher than the sum of atomic polarizabilities. These values will give approximate upper limits of the rate constants, 2.94 X 10^9 and 2.62 X 10^9 cc/molecules·sec for rubidium and cesium, which are about 3.5 times higher than our estimated rate constants.

Table V-4 The rate constant of the reaction
$M^+ + M_2 \rightarrow M_2^+ + M$ of rubidium and cesium

Element (M)	Rb	Cs
experimental condition		
T(° C)	360	342
P(mmHg)	0.193	0.199
time of 50% conversion (sec)	0.49×10^{-3}	0.67×10^{-3}
rate constant k [cc/molecules·sec]	0.79×10^{-9}	0.88×10^{-9}

2. Mobilities of rubidium and cesium ions in their parent vapors.

The measured values of the drift velocity, w_+ versus the electric field to pressure ratio, are shown in Figs. V.2, and 3. The pressure Po is the normalized pressure, i.e. $P_0 = 273\ P/T$, where T is the gas temperature. For comparison of present data with the drift velocity versus E/P_0 behavior predicted by Wannier,[48] lines of slope unity at low E/P_0 and one-half at high E/P_0 are shown in Fig. V.1 and 2. Wannier pointed out that for the low-field case the dominant ion-atom interaction is either the polarization interaction or resonance charge transfer interaction. Accordingly collisions between ion and atom are characterized by a constant mean free time and lead to a drift velocity varying directly with E/P_0. For the high-field case the short-range repulsion and resonance charge transfer becomes dominant, collisions are characterized by a constant mean free path and lead to a drift velocity varying with $(E/P_0)^{1/2}$.

Our data show that both rubidium and cesium ions in the range of our measurement are in the range of transition from slope one-half to one.

Figures V.4 and 5 shows a plot of the corresponding normalized mobility values. The mobility μ_o refers to a gas density of $2.69 \times 10^{+19}$ atoms/cc (equivalent to 760 Torr at 0°C). The zero-field mobility values for the ions observed in the present study as determined from Fig. V-3 and 4 are 0.20 cm/v.sec for Cs^+, 0.12 cm/v·sec for Cs^+, 0.29 cm/v·sec for Rb^+, and 0.18 cm/v·sec for Rb^+.

For Rb_2^+ and Cs_2^+ in the low-field case, the interaction with parent gas atoms is mainly the long-range polarization interaction $V(R) = -\frac{1}{2}\ \frac{\alpha e^2}{r^4}$, where α is the polarizability of the gas atom and r is the distance between the molecule-ion and the atom. The normalized mobility

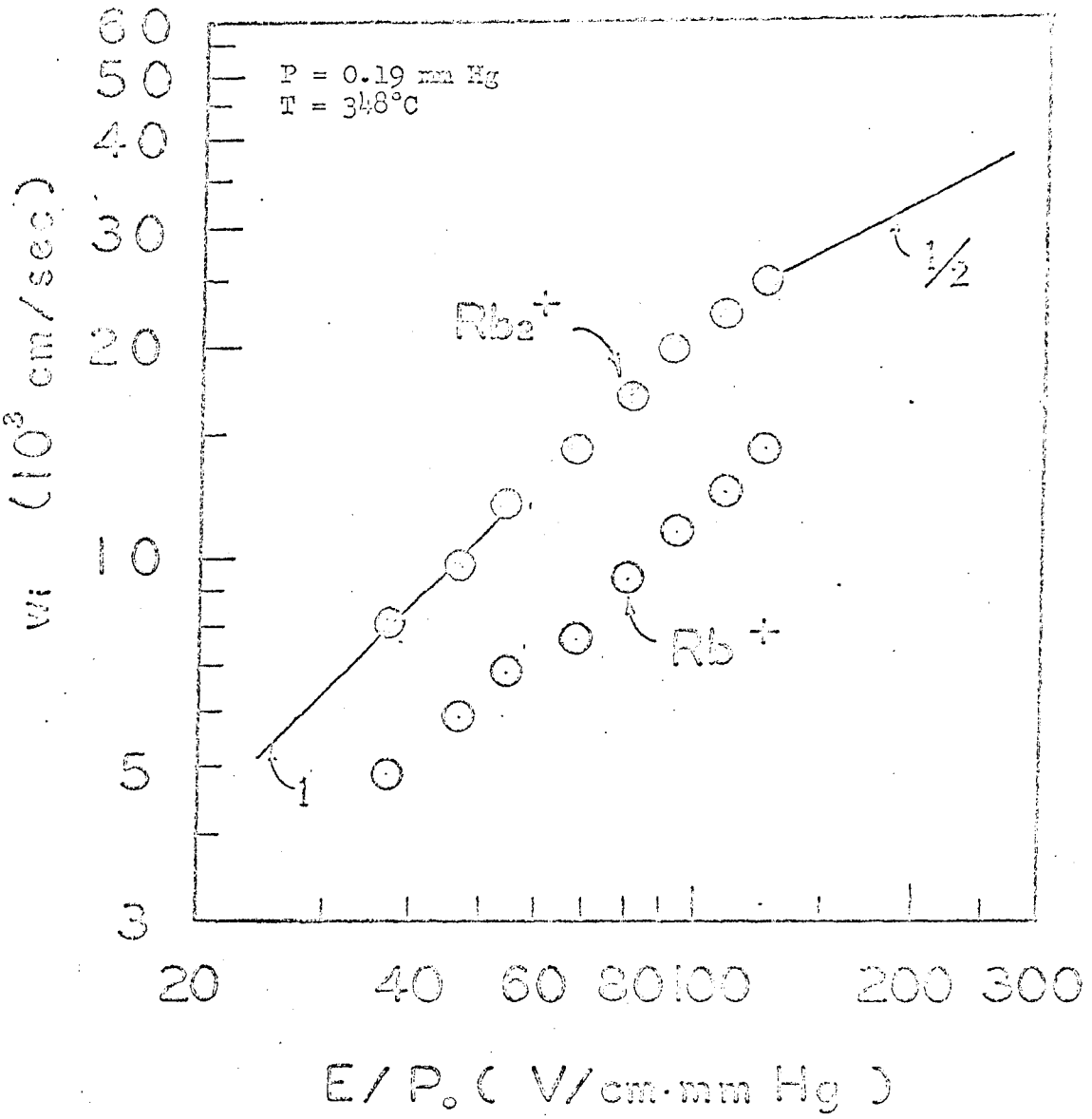

Fig. V-2. The variation of the drift velocities of Rb^+ and Rb_2^+ with E/P_0

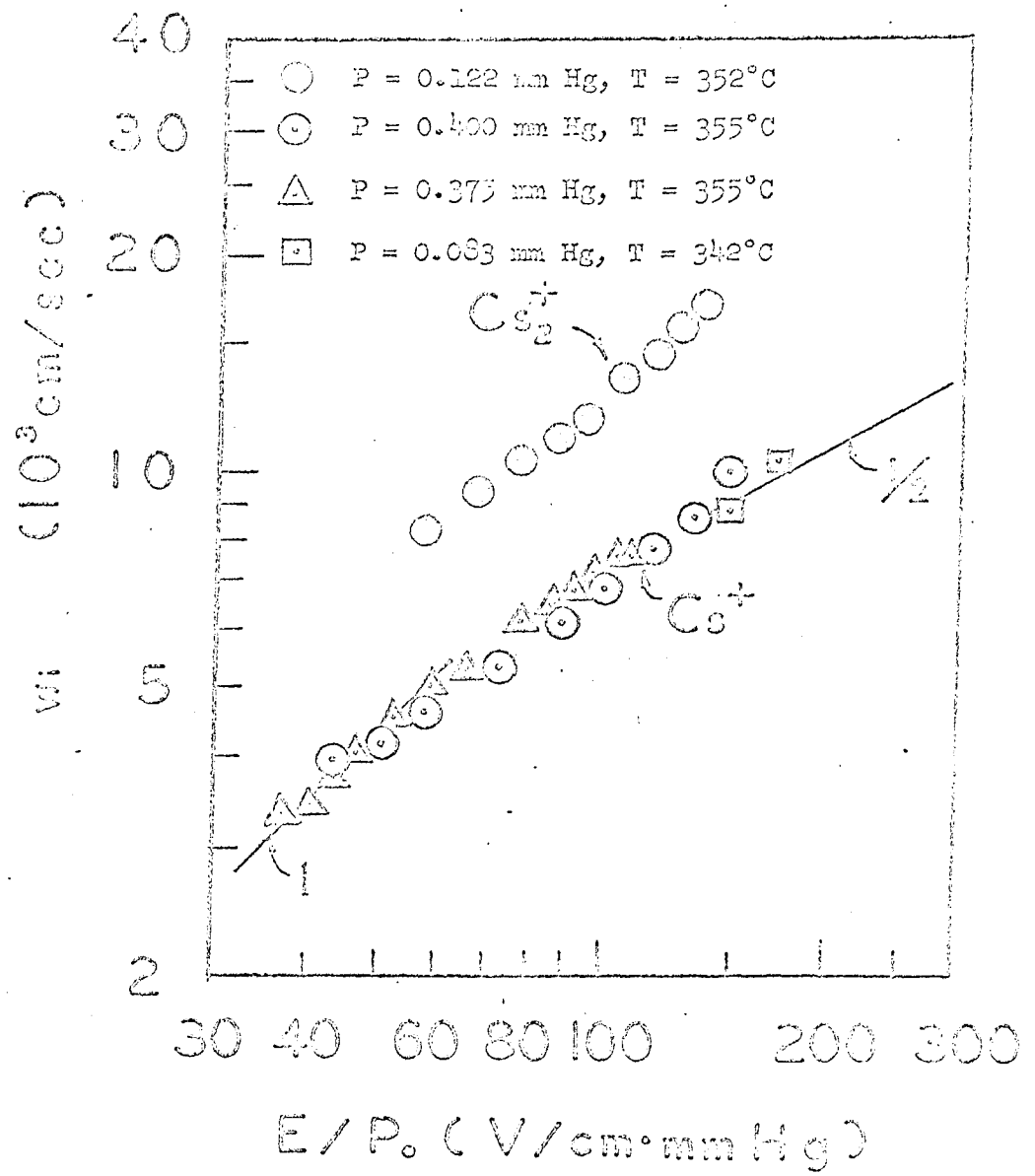

Fig. V-3. The variation of the drift velocities of Cs^+ and Cs_2^+ with E/P_0

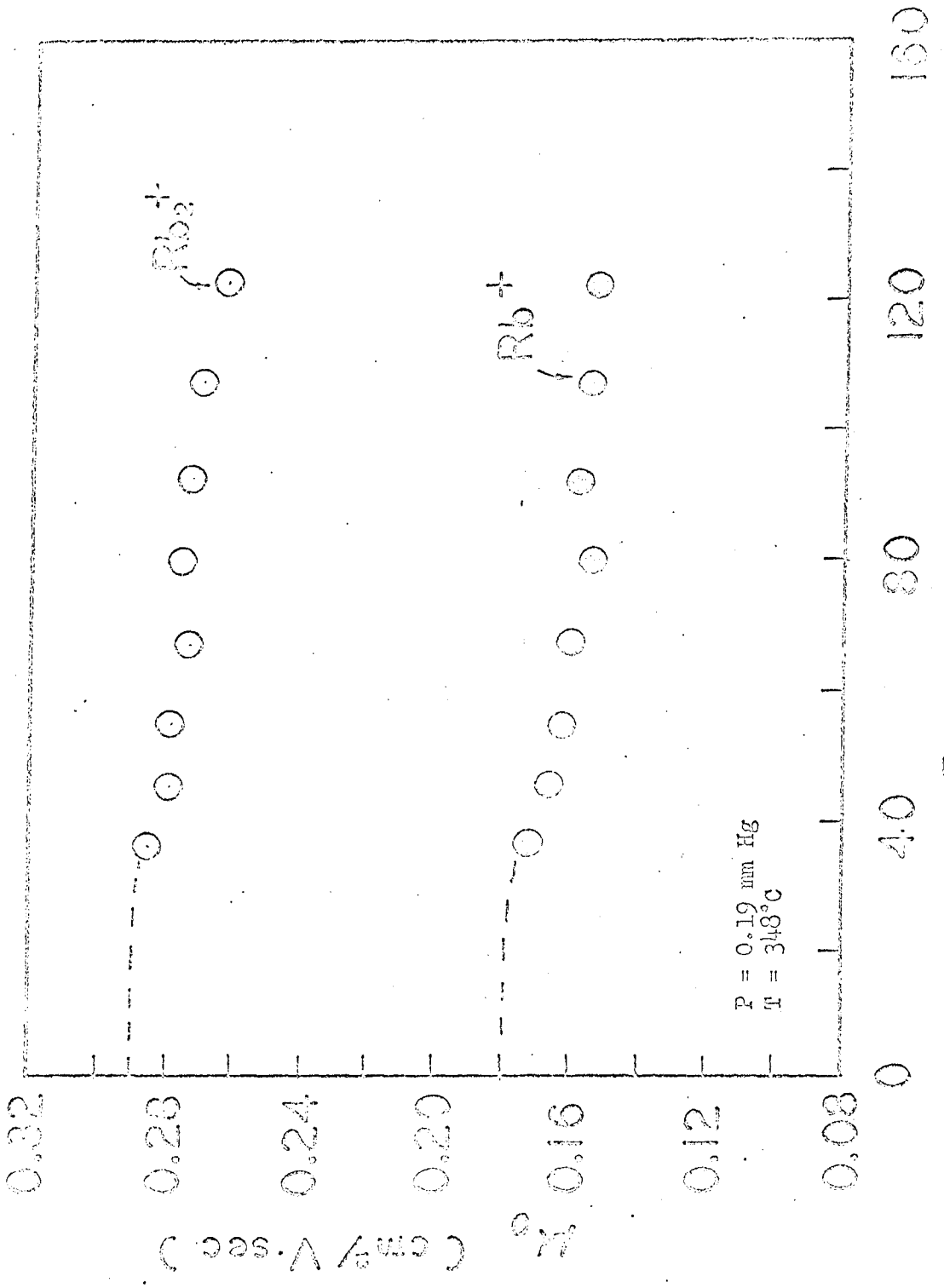

Fig. V-4. The variation of the normalized mobilities of Rb^+ and Rb_2^+ with E/P_o

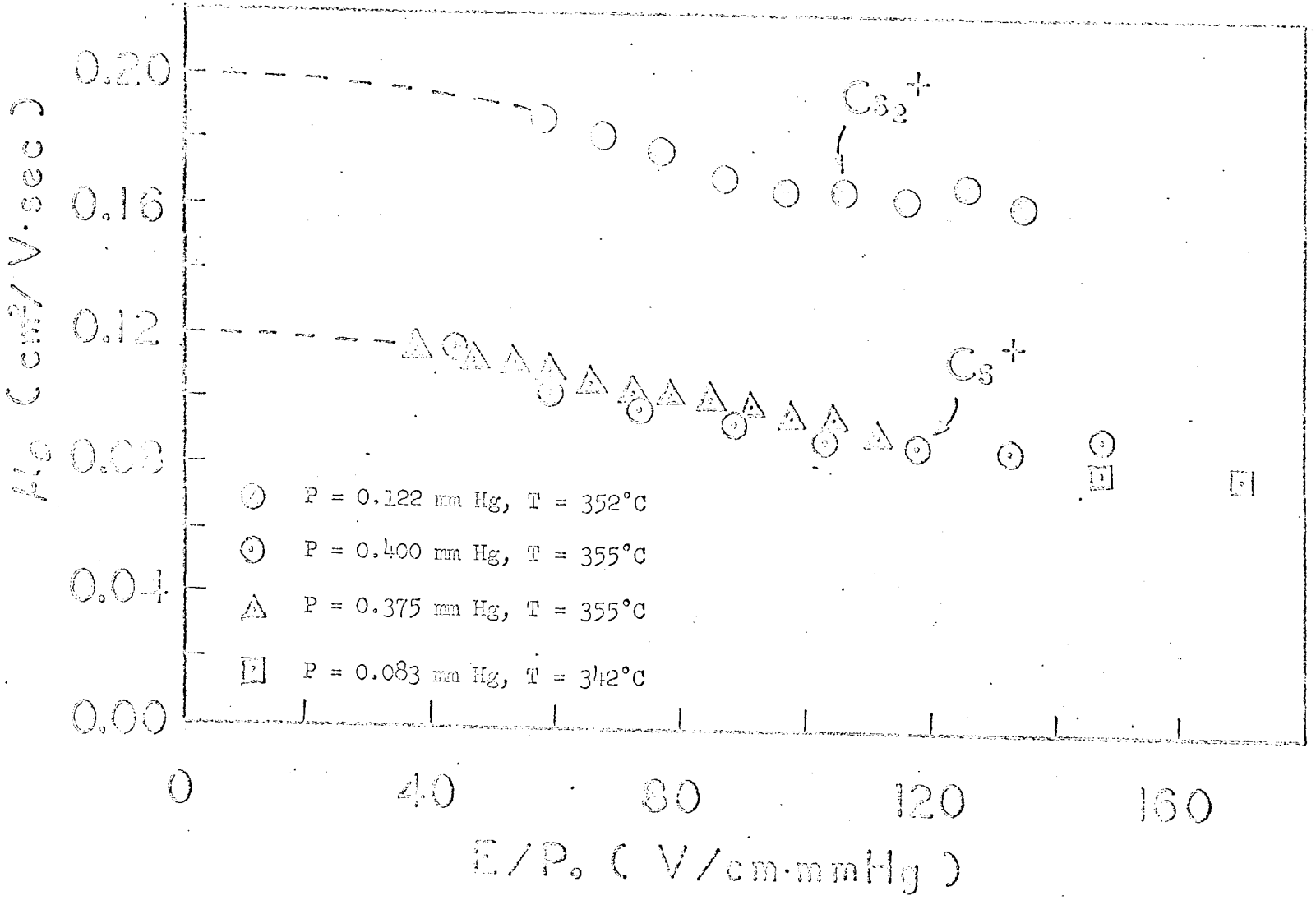

Fig. V-5. The variation of the normalized mobilities of Cs^+ and Cs_2^+ with E/P_0

in the first approximation is simply related to α and reduced mass of molecule-ion and gas atom μ and does not depend on temperature as was shown by Dargarno, McDowell and Williams[49] who found

$$\mu_o = \frac{35.9}{\sqrt{\alpha\,\mu}} \quad .$$

Our zero field mobility values for Rb_2^+ and Cs_2^+ correspond to the polarizability of 54.6×10^{-24} cm^3 for cesium atom and 39.8×10^{-24} cm^3 for rubidium at . These are in good agreement with the known polarizability of cesium $42 \sim 52.5 \times 10^{-24}$ cm^3 [50] and rubidium $40 \pm 5 \times 10^{-24}$ cm^3.[51] Our value of the normalized mobility of Cs_2^+ is in good agreement with Chanin and Steen's,[52] but the mobility of Cs^+ is considerably higher than their value of 0.075 cm/v·sec.

For Cs^+ and Rb^+, due to resonant charge exchange interaction, the normalized mobility is smaller than that of heavier diatomic molecule-ions. At present, experimental values of the charge transfer cross-section are not available at the low energies of interest in mobility measurements. Thus in order to calculate the mobility, the high-ion-energy data must be extrapolated down to low energies. This extrapolation involves several difficulties, arising from the errors in the high energy values as well as the magnitude of the energy range over which the extrapolation must be performed, and so does not offer reliable values. By using an approximate form of the charge-exchange cross section, Sheldon[53] has extrapolated four sets of independent experimental data of Cs^+ and subsequently calculated the corresponding mobilities. This extrapolation was performed assuming a variation of the cross section Q with relative ion-atom energy of the form

$$Q = (A - B \ln E)^2$$

where A and B are constants. The calculated normalized mobilities of Cs^+ in cesium vapor are 0.036, 0.055, 0.074, and 0.088 cm^2/volt·sec. Using the same procedure, we extrapolated the recent experimental data of Marino et al.[54] and calculated the normalized mobility of 0.0606 cm^2/volt·sec.

Theoretically, resonant charge exchange cross sections can be estimated by interpolating in terms of their ionization potentials.[55] The ratio of resonant charge exchange cross sections between Cs and Rb thus estimated is about 1.2. By considering their masses, we can expect the mobility ratio in the low-field limit to be about 1.5; this is in good agreement with our experimental results. From the same consideration, the mobility ratio between Xe^+ and Cs^+ would be about 4. The mobility of Xe^+ in xenon is known to be 0.6 cm^2/volt sec.[56] Our result of Cs^+ in cesium vapor will give a ratio of 5. It is a better agreement than the result of Chanin et al.[52] Their result gives a ratio of 8.

No comparison of the measured mobilities of Rb^+ and Rb_2^+ in their parent vapor can be made with other experimental results for there is no such measurement reported so far.

ACKNOWLEDGMENT

It is a pleasure to thank Professor Bruce H. Mahan for his guidance during the pursuit of this research. I also appreciate my wife Chinli for her encouragement and assistance.

This work was performed under the auspices of the United States Atomic Energy Commission.

REFERENCES

1. F. Mohler, P. Foote, and R. Chenault, Phys. Rev. 27, 37 (1926).
2. E. O. Lawrence and N. Edlefsen, Phys. Rev. 34, 233 (1929).
3. F. Mohler and C. Boeckner, Nat. Bur. Stand. J. Res. 5, 51 (1930).
4. K. Freudenberg, Zeit. f. Physik, 67, 417 (1931).
5. F. Mohler and C. Boeckner, Nat. Bur. Stand. J. Res. 5, 399 (1930).
6. H. M. James, J. Chem. Phys. 3, 9 (1935).
7. R. F. Barrow, N. Travis and C. V. Wright, Nature 187, 141 (1960).
8. E. W. Robertson and R. F. Barrow, Proc. Chem. Soc. 329 (1961).
9. E. H. S. Burhop and R. Marriott, Proc. Phys. Soc., London A69 (1956) 271.
10. R. A. Buckingham and A. Dalgarno, Proc. Roy. Soc. A213 (1952) 327, 506.
11. O. Klein and S. Rosseland, Z. Physik. 4, 46 (1921).
12. Mitchell and Zemansky, Resonance Radiation and Excited Atoms, Cambridge University Press (1934), p. 156.
13. H. Stuart, Z. Physik. 32, 262 (1925).
14. H. Beutler and B. Josephy, Z. Physik. 53 (1929) 744.
15. A. V. Phelps, Phys. Rev. 99 (1955) 1307.
16. E. E. Muschlitz and W. P. Sholette, University of Florida Rep. G.-5967, 1960.
17. M. A. Biondi, Phys. Rev. 82, 543 (1951).
18. B. Gudden, Lichtelektrische Erscheinungen, Springer-Verlag, Berlin, (1928) p. 226.
19. F. L. Mohler, C. Boeckner, J. Res. Natl. Bur. Std. 5, 51 (1930).
20. Z. Herman and V. Cermak, Nature 199, 4893, 588 (1962).

21. I. P. Bogdanova, I. Ceitsi, Opt. i Spectroskopiya 17, 1 (1964).

22. I. P. Bogdanova, O. P. Bochkova and S. E. Frish, Dokl. Akad. Nauk SSSR, 156,54 (1964); Soviet Phys.-Doklady 9, 370 (1964).

23. C. E. Melton and W. H. Hamill, J. Chem. Phys. 41, 1471 (1964).

24. D. R. Bates and H. S. W. Massey,Phil. Trans. A239, 269 (1943).

25. E. R. Bates, J. T. Lewis, Proc. Phys. Soc., London A68, 173 (1955).

26. D. R. Bates and T. J. M. Boyd, Proc. Phys. Soc., London A69, 910 (1956).

27. Mitchell and Zemansky, Resonance Radiation and Excited Atoms, Cambridge University Press (1934) p. 22.

28. L. M. Chanin and R. D. Steen, Phys. Rev. 132, 2554 (1963).

29. F. J. Comes, Z. Naturforsch. 17a, 1032 (1962).

30. E. A. Mason and J. T. Vanderslice, J. Chem. Phys. 29, 361 (1958).

31. G. Herzberg, Spectra of Diatomic Molecules, D. Van Nostrand, Inc., (1950).

32. P. N. Reagan, J. C. Browne and F. A. Matsen, Phys. Rev. 132, 304 (1963).

33. A. G. Gaydon, Proc. Phys. Soc. (London) 58, 525 (1946).

34. H. M. James, J. Chem. Phys. 3, 9 (1935).

35. J. Faulkner, J. Chem. Phys. 27, 32 (1957).

36. O. Sinanoglu and E. Mortenson, J. Chem. Phys. 34, 1078 (1961).

37. J. C. Browne, J. Chem. Phys. 42, 1428 (1965).

38. J. C. Browne, J. Chem. Phys. 41, 3495 (1964).

39. S. Franga and B. J. Ransil, J. Chem. Phys. 35, 669 (1961).

40. F. L. Arnot and J. C. Milligan, Proc. Roy. Soc. (London) A153, 359 (1935).

41. G. S. Kvater and T. G. Meister, Vestnik Leningradskogo Universiteta, No. 9, 137-158 (1952): Translation of this article is included in Optical Transition Probabilities, Israel Program for Scientific Translation.

42. O. Ruff and O. Johannsen, Ber. Chem. Ges. 38, 3601 (1905).

43. J. B. Jaylor and J. Langmuir, Phys. Rev. 51, 753 (1937).

44. G. I. Goldberg, Izvestiya Glavnoi Astronomicheskoi Observatorii 20 (156), 126-137 (1956).

45. See note (a) Table III-II (page 36).

46. The spectroscopic notation is that used by Herzberg. Note (c) Table III-II (page 36).

47. G. Gioumousis and P. P. Stevenson, J. Chem. Phys. 29, 294 (1958).

48. G. H. Wannier, Phys. Rev. 83, 281 (1951).

49. A. Dalgarno, M. R. C. McDowell and A. William, Phil. Trans. A250, 426 (1958).

50. G. E. Chamberlain and J. C. Zorn, Phys. Rev. 129, 677 (1963).

51. A. Salop, E. Pollack and B. Bederson, Phys. Rev. 124, 1431 (1961).

52. L. M. Chanin, R. D. Steen, Phys. Rev. 132, 2554 (1963).

53. J. W. Sheldon, J. Appl. Phys. 34, 444 (1963).

54. L. L. Marino, A. C. H. Smith, E. Caplinger, Phys. Rev. 128, 2243 (1962).

55. D. Rapp and W. E. Francis, J. Chem. Phys. 37, 2631 (1962).

56. R. N. Varney, Phys. Rev. 88, 362 (1952): L. M. Chanin and M. A. Biondi, Phys. Rev. 106, 473 (1957).

FIGURE CAPTIONS

Fig. II-1. Quenching curve for Hg resonance radiation.

Fig. II-2. Intensity of emission, divided by frequency and statistical weight, in arbitrary units, for levels of Na excited by mercury 6^3P_1 and 6^3P_0, as a function of energy of the Na level.

Fig. III-1 Schematic diagram of the experimental arrangement.

Fig. III-2 Side view of the photoionization cell and alkali metal filling system.

Fig. III-3 Phase angle (arbitrary units) as a function of photo-excitation energy for the cesium system. Experimental conditions: 6.67 volts/cm, 339 °C, 0.15 mm Hg. Ionization from the 8P state could be detected, but its phase could not be measured.

Fig. III-4 Phase angle (arbitrary units) as a function of photo-excitation energy for the rubidium system. Experimental conditions: Voltage as indicated, 339° C, 0.125 mm Hg. Ionization from the 7P state could be detected, but its phase could not be measured.

Fig. III-5 Phase angle (arbitrary units) as a function of photo-excitation energy for the potassium system. Experimental conditions: 2.67 volts/cm, 300°C, 0.068 mm Hg.

Fig. III-6. Ion current (arbitrary scale) as a function of electric field. Experimental conditions: 300 °C, 0.03 mm Hg.

Fig. V-1. The variation of vapor pressures of Rb and Cs with temperature.

Fig. V-2. The variation of the drift velocities of Rb^+ and Rb_2^+ with E/P_0.

Fig. V-3 The variation of the drift velocities of Cs^+ and Cs_2^+ with E/P_0.

Fig. V-4 The variation of the normalized mobilities of Rb^+ and Rb_2^+ with E/P_0.

Fig. V-5 The variation of the normalized mobilities of Cs^+ and Cs_2^+ with E/P_0.